VATNAJÖKULL:
Mass balance, meltwater drainage and surface velocity of the glacial year 2012_13

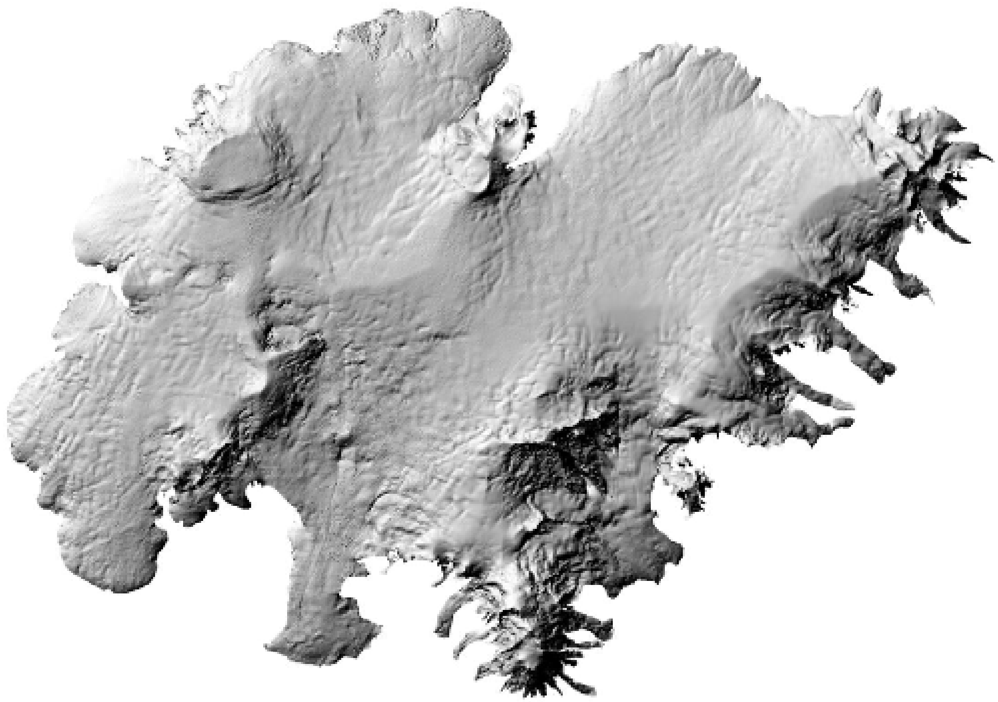

Institute of Earth Sciences
University of Iceland
and
National Power Company

Finnur Pálsson
Andri Gunnarsson
Þorsteinn Jónsson
Sveinbjörn Steinþórsson
Hlynur Skagfjörð Pálsson

RH-26-2013

Contents:

1. INTRODUCTION

In 1992 (glacial year 1991_1992) a program of mass balance measurements was started for Vatnajökull by the Science Institute University of Iceland (now Institute of Earth Sciences, IES) in collaboration with the National Power Company (NPC). For the first year the program was limited to the western part of the glacier, but then expanded to include the northern outlets as well. In 1996 this study was further expanded to include southern outlets, with support from The European Union (Framework IV - Environment and Climate, TEMBA project 1996-1997). This program was extended 1998–2000 with further support from EU (Framework IV - Environment and Climate, ICEMASS project, 1998-2000). In 2000-2002 NPC and IES continued the program. In 2003-2005 IES participated in a multinational research project, which was financially supported by The European Union (EVK2-CT-2002-00152 SPICE). IES was responsible for obtaining data sets for calibration of models of the mass balance and dynamics of Vatnajökull. This work was also supported by The National Power Company of Iceland and The National Road Authority, and is a continuation of the TEMBA-project of 1996-97 and ICEMASS project 1998-2001.

In 2012-2013 IES and NPC continued a similar program. Mass balance measurements on the southeast outlets Breiðamerkurjökull and Hoffellsjökull is financially supported by the National Road Authority.

The aim of the collaborative work of NPC and IES is to improve our understanding of the mass balance and melt water runoff from glaciers. This work in combination with energy balance measurements by NPC and IES on Vatnajökull will be used for calibration of models of the energy and mass balance of Vatnajökull.

This report describes the field measurements, GPS survey, the mass balance and melt water runoff for the glacial year 2012_13.

2. DIARY

January 30-31: winter mass balance measurements, maintenance of AWS's on Breiðamerkurjökull.
May 1 - 9: measurements of the winter balance
June 2 - 7: measurements of the winter balance.
October 1-8: summer balance measurements.

In all expeditions and short visits to the glacier the locations of mass balance stakes were measured with Kinematic GPS (or fast static GPS and a few with DGPS) for surface velocity calculation.

The following members of staff of the Institute of Earth Sciences, University of Iceland, carried out the fieldwork on Vatnajökull: Finnur Pálsson, Þorsteinn Jónsson, Sveinbjörn Steinþórsson and Ágúst Gunnlaugsson. Also Andri Gunnarsson (National Power Company) and Hlynur Skagfjörð Pálsson (Reykjavík Rescue Team). Members of the Iceland Glaciological Society assisted in the June fieldwork.

3. MASS BALANCE MEASUREMENTS

The purpose of the mass balance measurements is to describe the temporal and spatial distribution of the components of the mass balance. The mean annual values of the components and their variation from year to year are analyzed and related to meteoro-logical conditions and climatic variability. The results will be used in studies of changes in the glacier volume, estimates of meltwater contribution to glacial rivers, mass balance modeling, evaluation of altitudinal and regional variations of mass balance in response to climatic variations, and to assess the hydrometeorological and dynamic response of the ice cap to climate change.

The mass balance was determined by a stratigraphic method, measuring changes in thickness and density relative to the summer surface. The winter balance was estimated by drilling ice cores through the winter layer in the spring. Ablation was monitored from markers; snow stakes were put up on the glacier and wires were drilled down in the ablation area. The summer balance was measured in the autumn.

3.1 Methods

Measurements of the surface mass balance on a large ice cap like Vatnajökull are impractical in terms of cost with conventional techniques and sampling density that are typically used on small glaciers. The spatial variability of the mass balance may, however, be predictable on the flat large outlets of such an ice cap given data on several profiles extending over the elevation range of the glacier. The precipitation generally increases with elevation and decreases with the distance from the coast, but both the distribution of snowfall and redistribution of snow by drift depend on the prevailing wind direction during the winter. The summer melting depends mainly on the altitude and the albedo of the glacier surface. Therefore, we have used observations along a limited number of flowlines, which span the elevation range of the outlets to assess aerial estimates of surface mass balance. Each profile describes the variation with elevation, but together they also describe the lateral variation of the mass balance. Recently, modern over-snow vehicles and helicopters have allowed fast traverses to ensure successful fieldwork in spite of frequently poor weather conditions. The error for individual point measurement is estimate ~30 cm_{we} for both summer and winter balance. The error for the area integral of mass balance is however considered smaller, since the error for individual survey sites is independent.

The winter mass balance (b_w) is defined as the mass of snow accumulated during the winter months, the summer balance (b_s) is the mass balance during the summer, and the net balance (b_n) is defined as their sum. The specific mass balance is expressed in terms of the equivalent thickness of water. All mass balance components apply to a time interval between given measurement dates, which are not fixed from one year to another. The dates in the autumn are separated by approximately one calendar year, which roughly coincides with the glaciological year defined as October 1st to September 30th. Snow cores are drilled in April-May through the winter layer and profiles of the density are measured. The summer balance is derived in the autumn from measurements of the changes in the snow core density during the summer in the accumulation area and from readings at stakes and wires drilled into the ice in the ablation areas.

Digital maps are created for winter, summer and net balance for the whole ice cap based on site measurements. The mass balance is calculated over both the ice and water drainage basins. The summer balance over the water basin is an estimate of meltwater contribution to rivers and groundwater storage. This estimate, however, does not include precipitation that falls as rain on the glacier or snow, which falls and melts during the summer. The meltwater contribution is compared with river runoff at stream flow gauges closest to the glacier. For this comparison, we define the glaciological year from the start of October to the end of September and the period draining meltwater from the glacier during the summer from June through September. It would be misleading to include May in the summer period because runoff from the glacier melt in May is delayed due to refreezing during elimination of the cold wave.

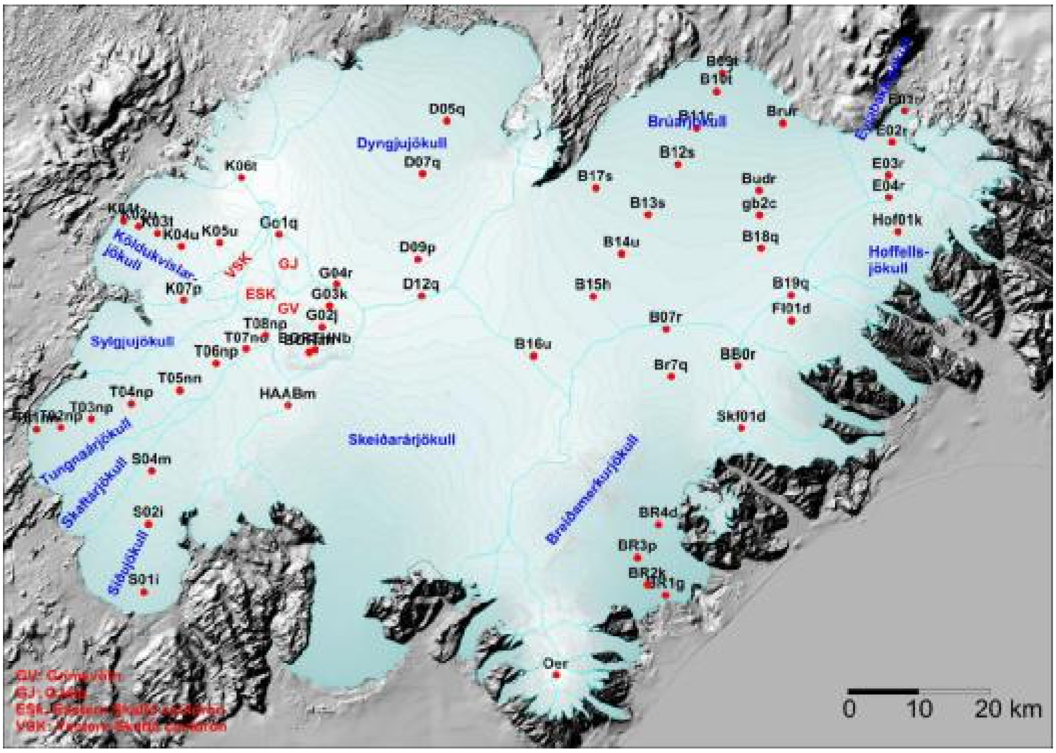

Figure 1. Outlets of Vatnajökull and location of mass balance measurement sites 2012_13.

3. 2 Results of mass balance measurements.

Mass balance measurements were done at 58 sites in spring 2013 (Fig. 1). The specific mass balance at individual sites is shown in Fig. 2. Most sites are on central flow lines at individual outlets. The specific mass balance along flow lines is given in Fig. 3 as a function of elevation for each glacier outlet: Síðujökull, Tungnaárjökull, Dyngju-jökull, Köldukvíslarjökull, Brúarjökull (west and east), Eyja-bakkajökull, Hoffellsjökull and Breiðamerkurjökull.

Digital maps for winter, summer and net balance are shown in Figure 4. Although no balance measurements are available for Skeiðarárjökull, the balance has been estimated by interpolating the balance values from the neighboring outlets, based on our experience from previous years. The mass balance of individual large outlets is discussed in the following

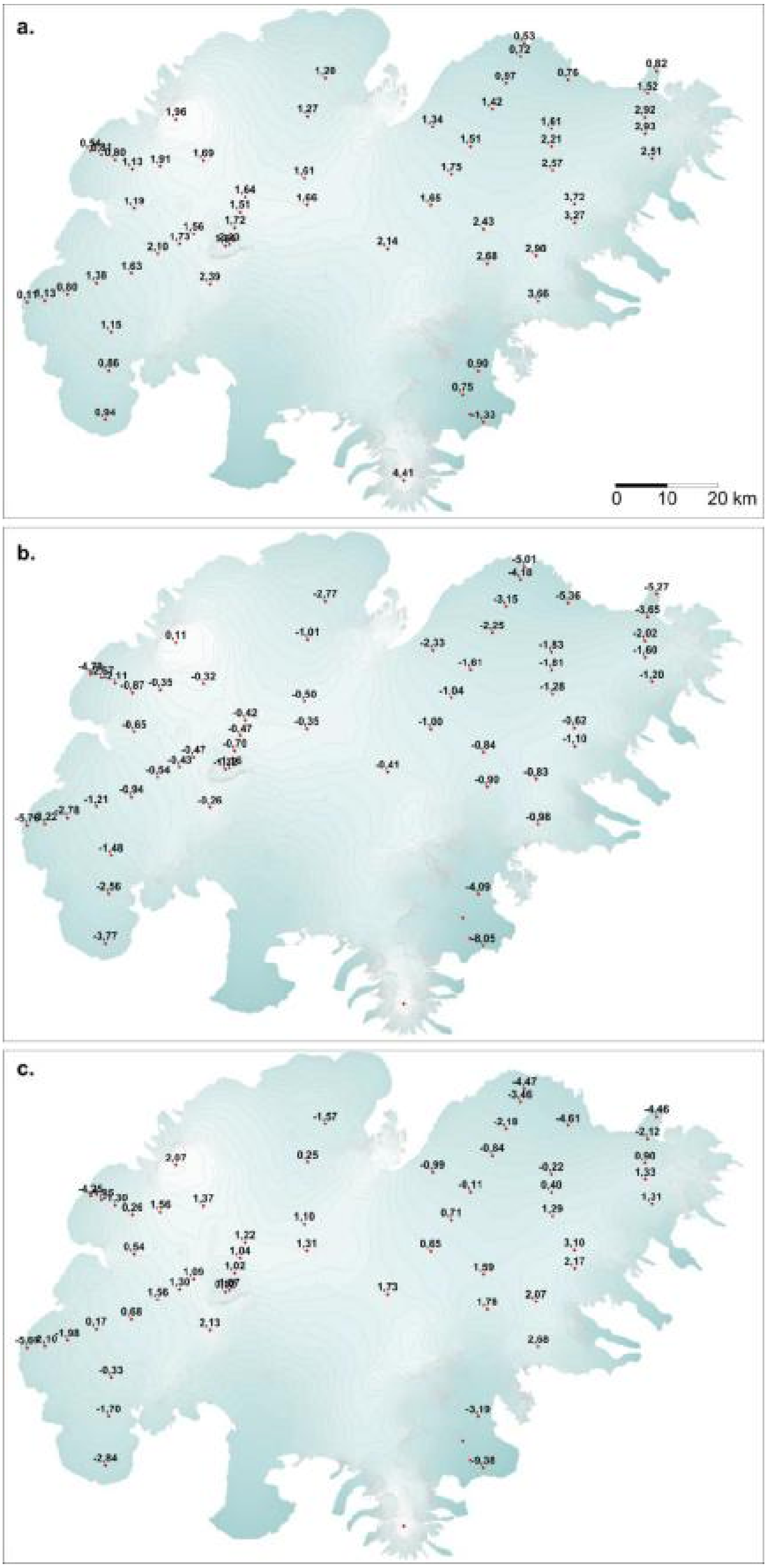

Figure 2. Maps showing point values of specific mass balance in m water equivalent (m_{we}), 2012_13. a. winter, b. summer, c. net balance.

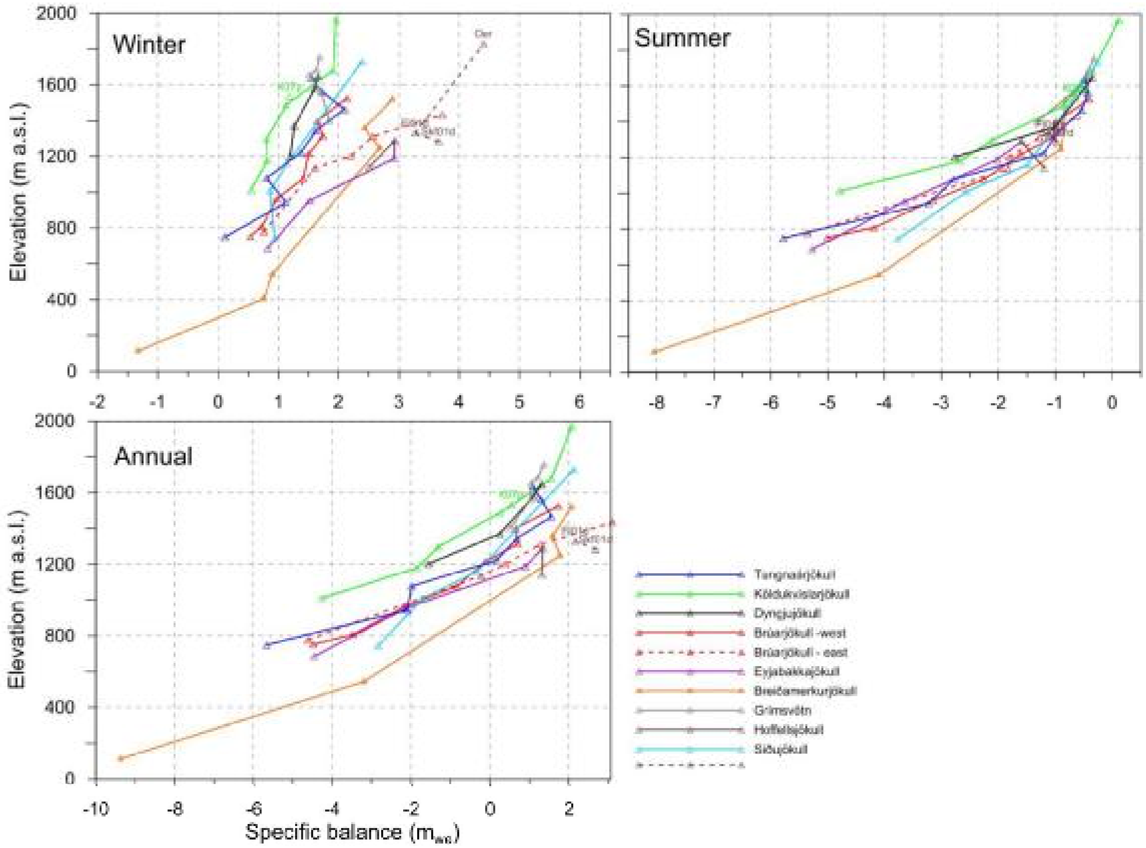

Figure 3a. Specific mass balance (m_{we}), along all mass balance profiles 2012_13.

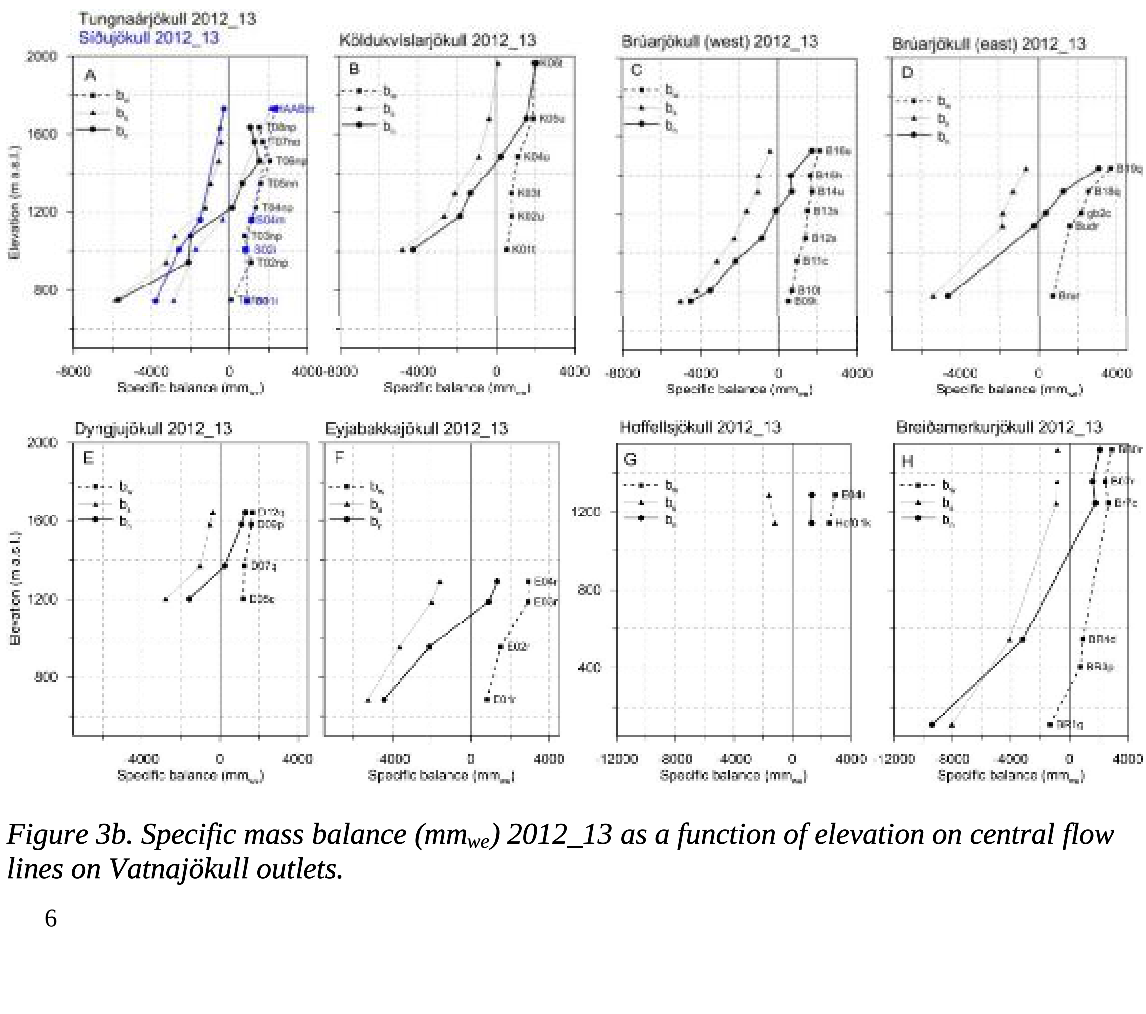

Figure 3b. Specific mass balance (mm_{we}) 2012_13 as a function of elevation on central flow lines on Vatnajökull outlets.

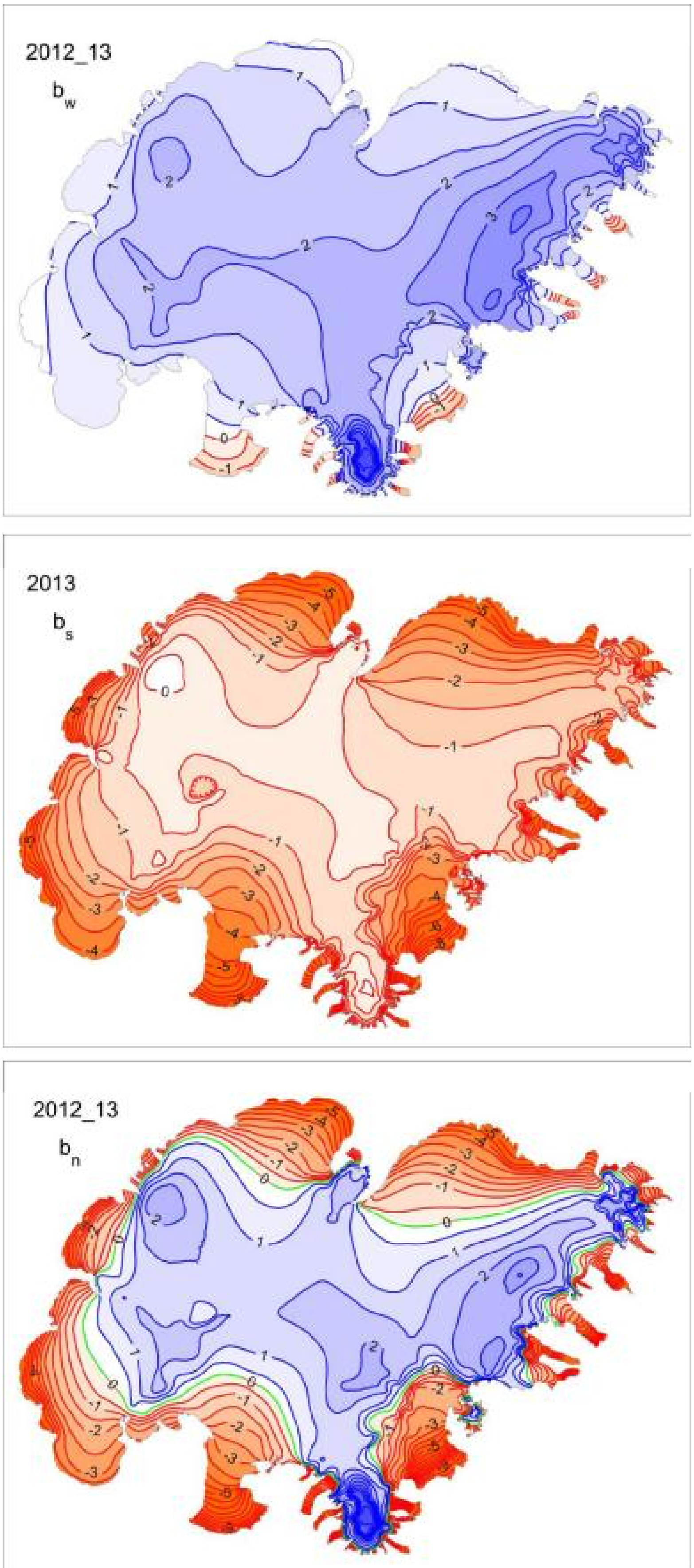

Figure 4. Specific mass balance (m_{we}) maps of Vatnajökull 2012_13. Top: winter, Centre: summer, Bottom: net balance.

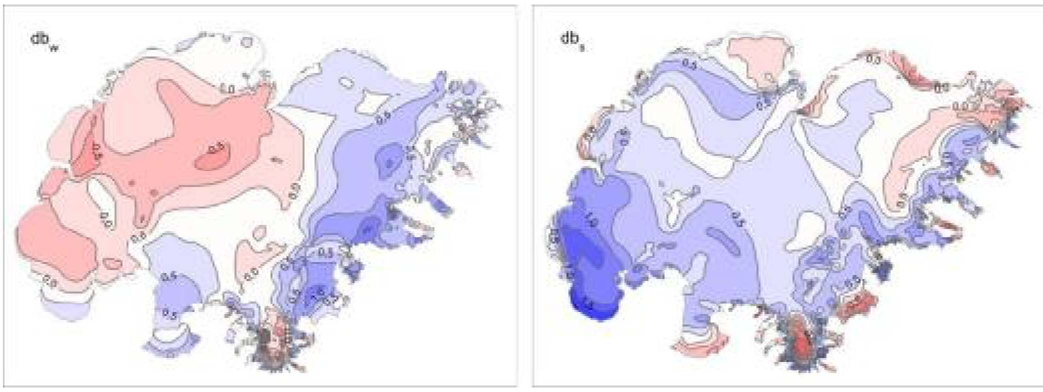

Figure 5. The left frame shows the difference between winter balance in 2012_13 and the average winter balance 1995_96 to 2011_12. (Positive (blue) is higher than average). The left frame shows the difference between summer balance in 2013 and the average summer balance 1996 to 2012. (Negative (red) is higher than average ablation).

subsections. A DEM of Vatnajökull mostly based on SPOT5 satellite images in 2010, and partly from LiDAR survey 2010, is used for surface area distribution and delineation of ice divides for individual outlets and catchments.

September 2012 was a stormy month, a northern snow blizzard in the second week delivered a thick snow layer N and NE Iceland, and some snow was accumulated on Vatnajökull, ablation came to an abrupt halt. October was calm, colder than average in the east. November was wet and stormy, but the snow cover in the highland west and north of Vatnajökull was thin (see MODIS images in Appendix F). First half of December was rather calm but the latter half was stormy and high precipitation in the north and east. January and February were exceptionally warm and wet, especially in south and west Iceland. Most of March was rather calm and dry, with a cold spell. April was cold and calm, and dry in the southeast. May was wet, yielding the highest precipitation in Höfn í Hornafirði since 1989. In May only 1 day is cloud free on Vatnajökull is seen in the MODIS images (Appendix F). Figure5, left, shows less than average snow cover in W and NW Vatnajökull, but higher than average accumulation in the S and E. Exceptionally high accumulation at the accumulation areas of Brúarjökull; Eyjabakkajökull and SE outlets reflects snowfall in SE, E, and NE wind directions. The thicker than average snow cover in Brúarjökull ablation zone delays summer ablation there. Inspection of the MODIS monthly overview of the summer months in Appendix F shows that days with clear skies over Vatnajökull were 1 in May, ~6 in June, ~7 in July most of them in latter half of the month, ~3 in August. This indicates that short wave radiation to towards the glacier surface was limited, resulting in lower than average ablation. However in June dust from the highland was blown over the northern outlets, lowering the albedo and increasing ablation. The summer months were rather warm but wet and cloudy in W and S Iceland. July and August were warm and sunny in E and NE Iceland; this also applies to the Northern and some of the SE outlets of Vatnajökull. September was stormy and wet, ablation came to a halt early.

All this resulted lower than average ablation on Vatnajökull (see fig. 5) except in the ablation zones of the northern outlets, and accumulation zones in the east.

(Information about weather is from the web site of the Iceland Met Office written by Trausti Jónsson).

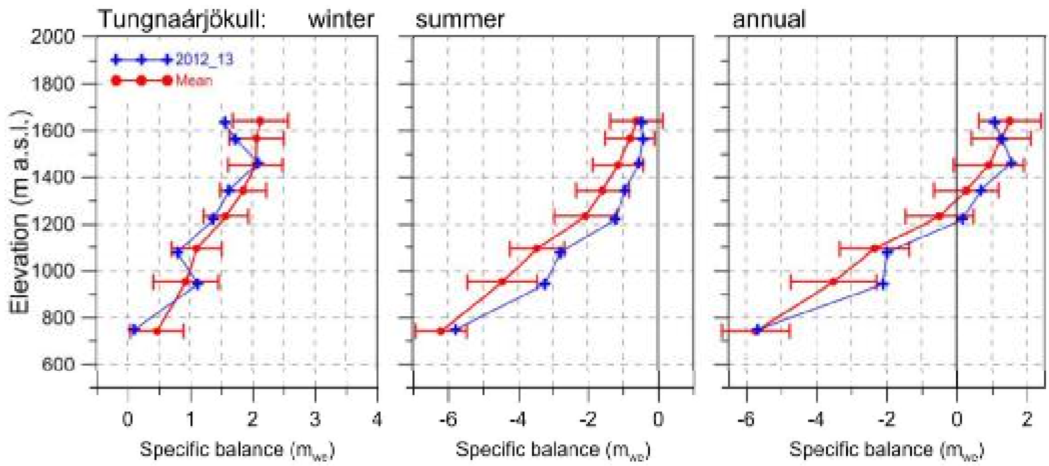

Figure 6. Mass balance at a central flow line of Tungnaárjökull 2012_13, and average mass balance 1991_92 to 2011_12.

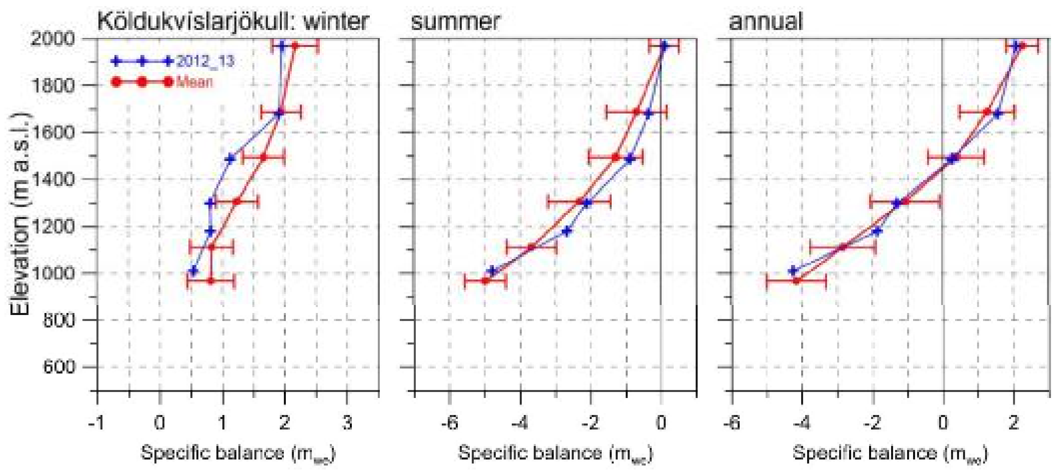

Figure 7. Mass balance at a central flow line of Köldukvíslarjökull 2012_13, and average mass balance 1991_92 to 2011_12.

3.2.1 Tungnaárjökull.

Area = 345 km^2
B_w= 0.41 km^3 ; b_w = 1.18 m
B_s = -0.69 km^3 ; b_s = -1.99 m
B_n = -0.28 km^3 ; b_n = -0.81 m
ELA = 1210 m (at profile)
AAR = 49 %

(The terms are defined at the foot of this page)

Variation of mass balance along a central flow line on Tungnaárjökull is shown in Fig. 6. The winter balance was lower than average at most sites of the survey sites. Winter balance was 80% of the average, the prevailing precipitation direction was from SE to NE, western Vatnajökull was somewhat shadowed by the topography. Summer melting was almost 1 std. dev. at all survey sites, except the top site, the summer was wet and cloudy in this region. The total ablation was only 75% of the average during the survey period. The net balance was negative the 19th year in a row; the loss was 0.3 m_{we} less than average during the survey period, (69% of than average).

3.2.2 Köldukvíslarjökull

Area = 301 km^2
B_w = 0.36 km^3 ; b_w = 1.19 m
B_s = -0.53 km^3 ; b_s = -1.75 m
B_n = -0.17 km^3 ; b_n = -0.56 m
ELA = 1450 m (at profile)
AAR = 48 %

B_w,B_s and B_n are water equivalent volumes of winter, summer and net balance, ELA the equilibrium line altitude, and AAR is the accumulation area ratio.

Variation of mass balance along a central flow line on Köldukvíslarjökull is shown in Fig. 7. Accumulation was about one st.var. less than average except the highest survey sites, where it was close to average. The winter balance was about 82% of the average since 1991_92. The summer melt was less than average at all sites, the cold period in spring and some snowfall during the summer in the upper regions explains this. In total the summer balance was 88% of the average. The net balance was negative the 19th year in a row, mass loss was 5% over the average during the survey period (by 0.03 m_{we}).

3.2.3 Dyngjujökull

Area = 1064 km^2
B_w= 1.47 km^3 ; b_w= 1.38 m
B_s = -1.71 km^3 ; b_s = -1.61 m
B_n = 0.24 km^3 ; b_n = -0.23 m
ELA = 1345 m (at profile)
AAR = 63 %

Variation of mass balance along a flow line on Dyngjujökull is shown on Fig. 8. Mass balance is not measured at the lowest elevations, but assumed to be similar (as a function of elevation) to that of Brúarjökull and Köldukvíslarjökull. The winter balance in 2010_11 was more than std.var. lower than average at the upper survey sites, but close to average at 1200 m, and almost nothing was accumulated in the ablation zone (no sites but this is obvious from the MODIS images in appendix F.) In total the winter balance was slightly (3%) less than average.
The summer ablation was close to average at all sites. The net balance was negative, about two times the average. Dyngjujökull is the outlet of Vatnajökull that during the survey period has often had mass balance close to zero, and the net balance has been slightly positive in some years of the two decade period of continuous mass loss for Vatnajökull as a whole.

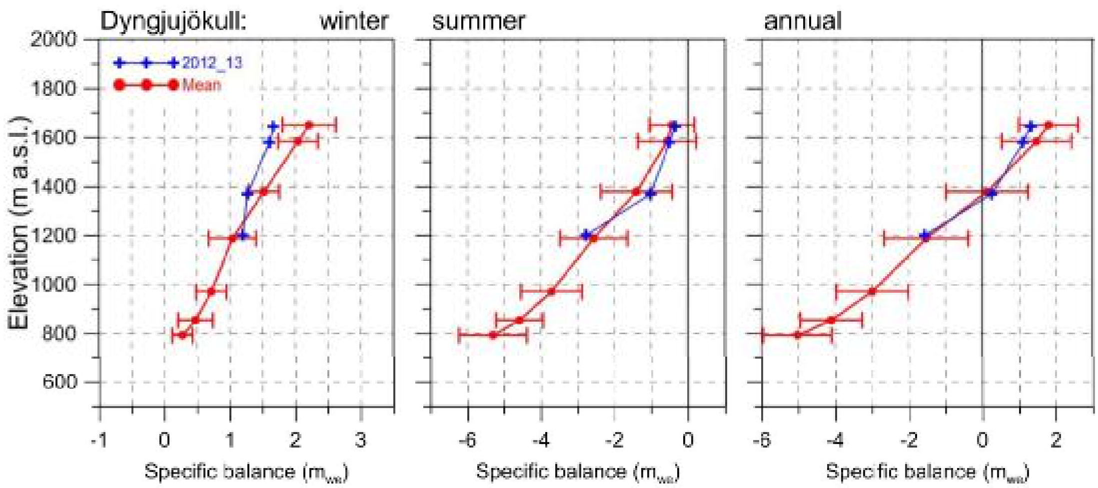

Figure 8. Mass balance at a central flow line on Dyngjujökull 2012_13, and average mass balance 1991_92 to 2011_12 (except 1998_99 – 2003_04 at all but the top elevation).

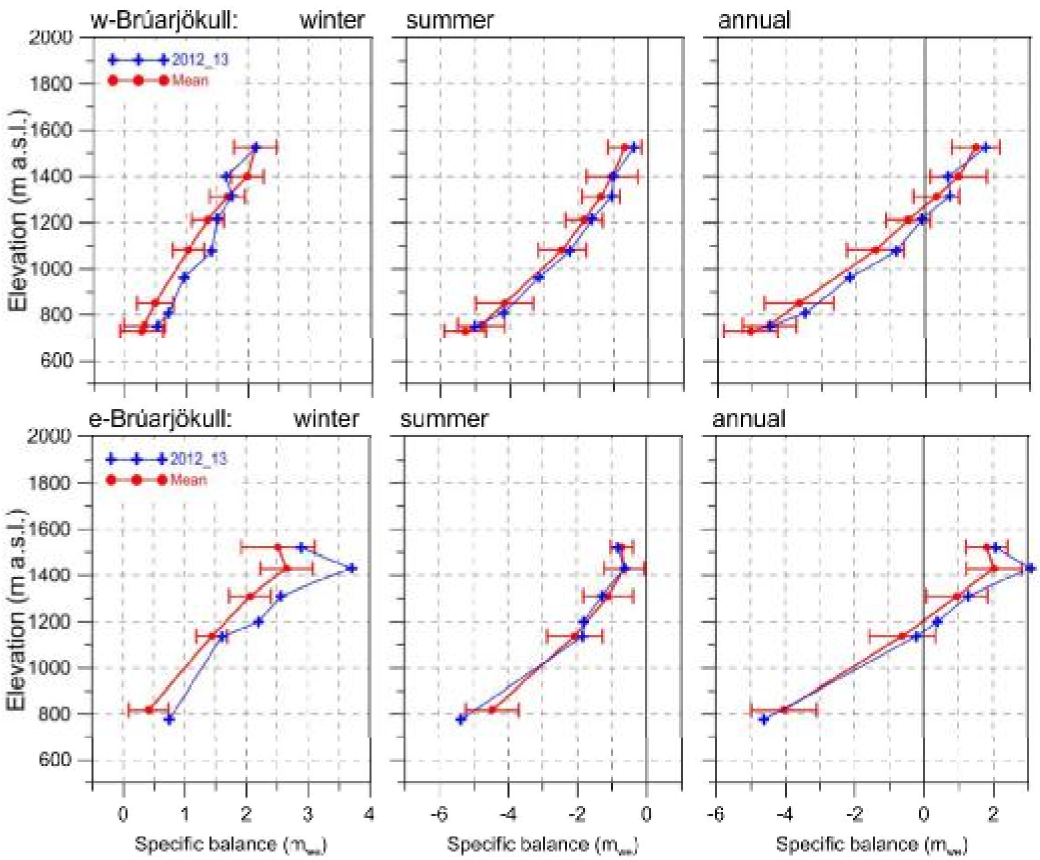

Figure 9. Mass balance at two flow lines on Brúarjökull 2012_13, and average mass balance 1992_93 to 2011_12.

3.2.4 Brúarjökull

Area = 1526 km^2
B_w= 2.65 km^3 ; b_w = 1.74 m
B_s = -2.76 km^3 ; b_s = -1.81 m
B_n = -0.11 km^3 ; b_n = -0.07 m
ELA = 1230 m (western flow line)
ELA = 1160 m (eastern flow line)
AAR = 61 %

Variation of mass balance along two flow lines on Brúarjökull is shown on Fig. 9. At all the lower (below ~1100m) survey sites accumulation was significantly (almost 1 std. dev.) more than average, also in the eastern part of the accumulation zone. But in the large area between ~1300-1500 m of the western part accumulation was close to average. This reflects the prevailing Eastern wind direction in precipitation events. The total winter balance higher (13%) than average. The thick snow cover of the ablation zone, delayed ablation in the ablation zone, but this effect was to a large extent compensated by dirt blown over most of Brúarjökull from the snow free highland in June (see Appendix F., images for June - August), that lowered the surface albedo. In the latter half of July and first half of August and there were many days of relatively clear skies, and warm weather; high ablation rates during this period. The resulting summer ablation was about 93% of the average. The net mass loss was negative; close to the average of the survey period (97%). During the survey period, there have been 5 years of positive balance, 16 with negative balance.

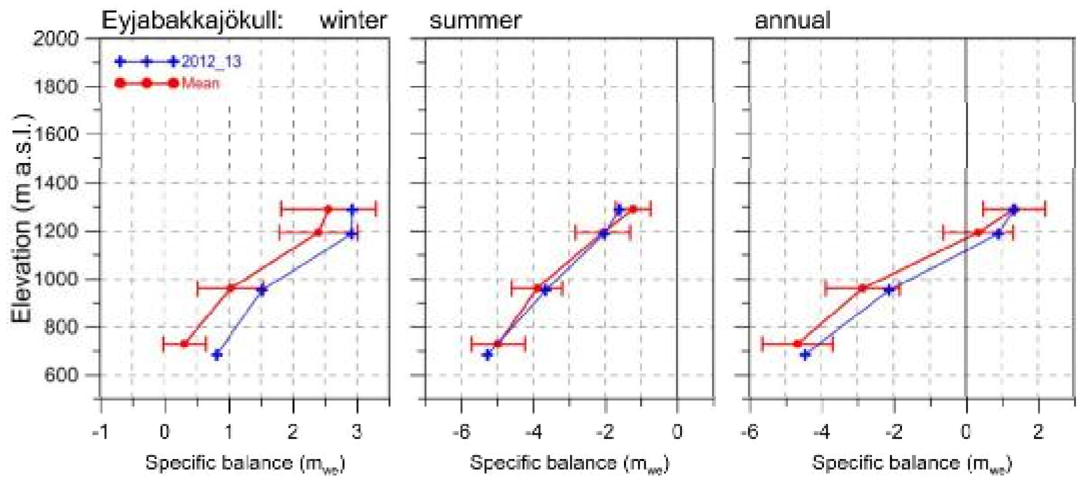

Figure 10. Mass balance at a central flow line of Eyjabakkajökull 2012_13 and average mass balance 1995_96 to 2011_12.

3.2.5 Eyjabakkajökull

Area = 112 km^2
B_w= 0.25 km^3 ; b_w = 2.21 m
B_s = -0.30 km^3 ; b_s = -2.71 m
B_n = -0.05 km^3 ; b_n = -0.50 m
ELA = 1120 m (at profile)
AAR = 49 %

Variation of mass balance along a central flow line on Eyjabakkajökull is shown on Fig. 10. As on E-Brúarjökull the winter balance was more than 1 std. var. higher than average at all survey sites; in total the winter balance was 27% higher than average. Summer ablation was close to average, in spite of late start of the ablation season, dirt enhanced ablation, and the weather in late July, early August was warm and sunny (see. Appenix F). The total ablation was 98% of the average. The annual balance was negative, but only by 50% of the average since 1995_96.

3.2.6 Breiðamerkurjökull

Area = 938 km^2
B_w= 1.75 km^3 ; b_w = 1.87 m
B_s = -1.99 km^3 ; b_s = -2.13 m
B_n = -0.24 km^3 ; b_n= -0.26 m
ELA = 995 m (at profile)
AAR = 62 %

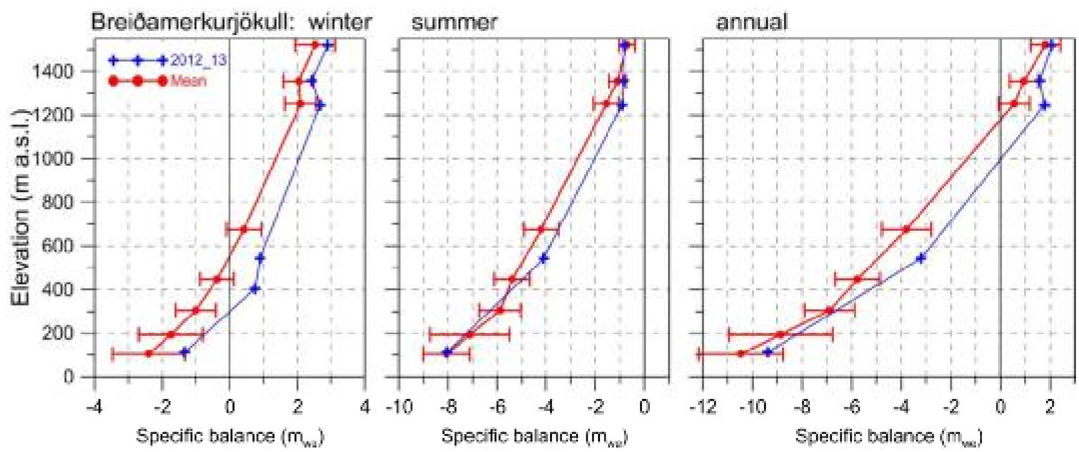

Figure 11. Mass balance at a central flow line of Breiðamerkurjökull 2012_13, and average mass balance 1995_96 to 2011_12.

Variation of mass balance along a central flow line on Breiðamerkur-jökull is shown on Fig. 11. The winter was rather cold and with high precipitation in the SE. Snow accumulation was about 1 std. dev. over average in the upper area. In the lower area accumulation was close to 1.5 std. dev. higher than average. The winter ablation at the lowest survey sites was also significantly less than average. The winter balance was 35% above average. Although latter half of summer was warm and sunny in the region, total ablation was only 82% of the average. The resulting net balance was negative but only 21% of the average. This is the closest to zero net balance on Breiðamerkurjökull during the survey period.

3.2.7 Síðujökull

Area = 430 km^2
B_w= 0.56 km^3 ; b_w = 1.29 m
B_s = -0.87 km^3 ; b_s = -2.02 m
B_n = -0.31 km^3 ; b_n= -0.73 m
ELA = 1235 m (at profile)
AAR = 43 %

Variation of mass balance along a central flow line on Síðujökull is

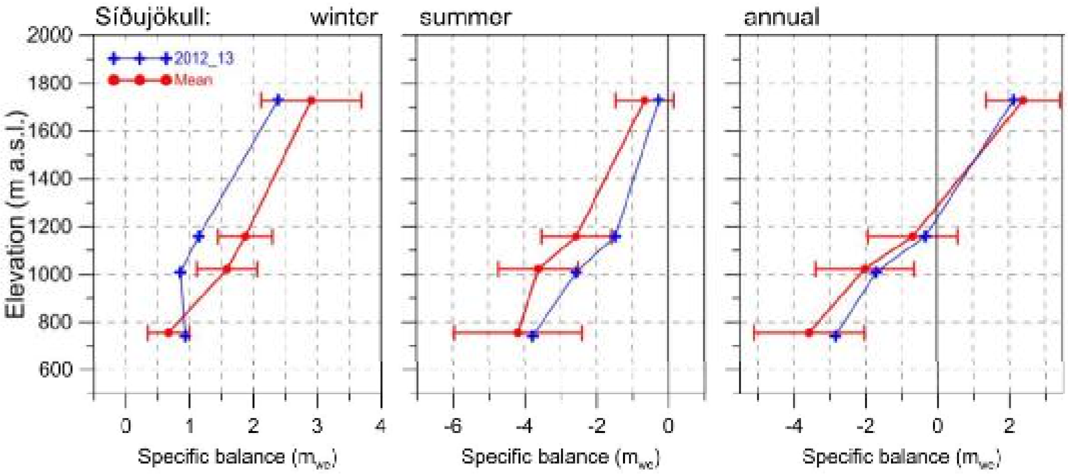

Figure 12. Mass balance at a central flow line of Síðujökull 2012_13, and average mass balance 2004_05 to 2011_12.

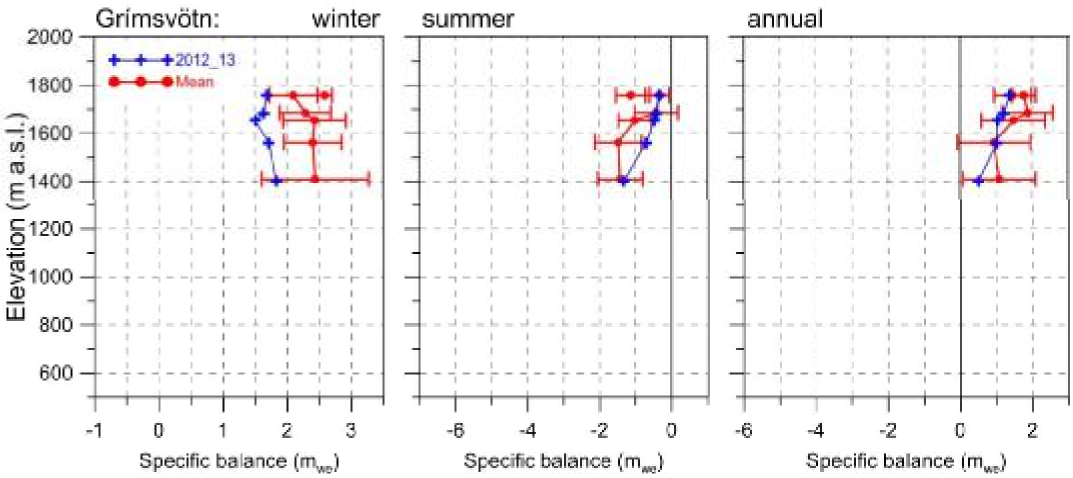

Figure 13. Mass balance at a central flow line towards Grímsvötn 2012_13, and average mass balance 1991_92 to 2011_12.

shown on Fig. 12. Snow accumulation much less than average in the upper area, but much higher than average (more than std. dev.) in the lowest area, the precipitation in SE wind directions did reach there. The total winter balance was 87% of the average. As on Tungnaárjökull the summer weather in this region was wet and cloudy, ablation was ~1 std. var. less than average; summer balance was only 67% of the average. The net balance was negative but only by half of the average.

3.2.6 Grímsvötn-Gjálp

Area = 174 km^2
B_w= 0.34 km^3 ; b_w = 1.92 m
B_s = -0.10 km^3 ; b_s = -0.60 m
B_n = 0.23 km^3 ; b_n= 1.32 m
ELA = 1250 m (at profile)
AAR = 47%

Variation of mass balance close to a central flow line from Bárðarbunga towards Grímsvötn center is shown on Fig. 13. Snow accumulation was more than 1std. dev. lower than average at all survey sites except the lowest. The winter balance was only 85% of the average. Ablation was less than average at all survey sites; then summer balance ~87% of the average. The net balance was positive, by 83% of the average of the survey period.

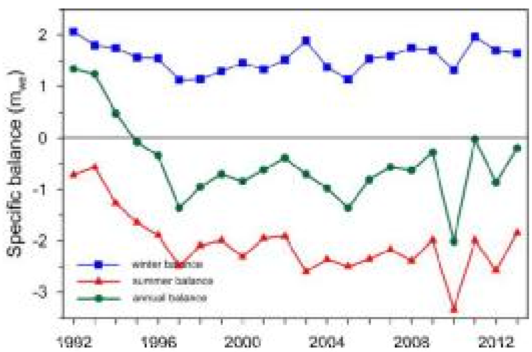

Figure 14. Specific mass balance record for Vatnajökull 1991_92 – 2012_13.

3.3 The mass balance record for Vatnajökull.

From the digital maps the total volumes of winter, summer and net balance have been calculated by integration (appendix D, gives balance values as a function of elevation) and are as follows:

B_w= 13.13 km^3 ; b_w = 1.65 m
B_s = -14.71 km^3 ; b_s = -1.85 m
B_n = -1.58 km^3 ; b_n = -0.20 m
AAR = 60%

Most of the winter was wet, with prevailing SE-E and NE winds. This lead to much higher than average snow accumulation on E-Vatnajökull, but less than average on W-Vatnajökull. The total winter balance was 13% over the average (over the observation period 1991_92-2011_12, Fig. 14). The 0 mass balance turnover for Vatnajökull (current topography) is close to 13.4 km^3 (1.64 m w. eq.) and the winter balance 2011_12 is about 7% lower. On W-Vatnajökull there summer was cloudy and wet, ablation there was less than average. The relatively long periods of clear skies and warm weather, in late summer,

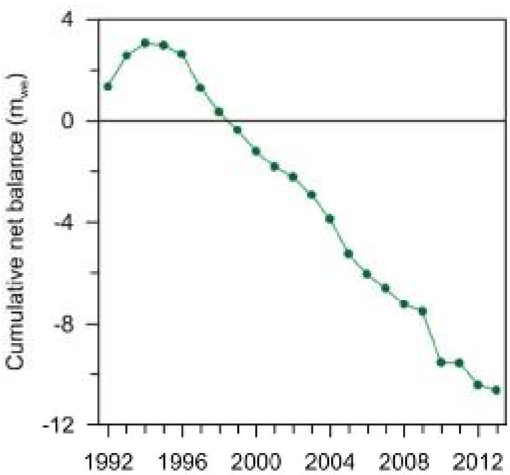

Figure 15. Cumalative specific mass balance of Vatnajökull 1991_92 – 2012_13.

combined with dirt blown over the glacier in the dry periods in June, enhanced ablation in E and N-Vatnajökull. This resulted in total summer balance ~92% of the average over the survey period, 10% higher than for zero balance turnover. The net balance was negative, however the mass loss was only 27% of the average loss (-0.75 m) of the past 18 consecutive years of negative balance.

The glacial year of 2012_13 was the 19th in a row with negative mass balance for Vatnajökull (Fig. 14, Fig. 15), contributing to a total loss of 13.7m_{we} (ice volume of ~122 km^3) since 1994_95.

The temporal variability of mass balance for different outlets is shown in Fig. 16. The greatest variability of the winter balance is for Eyjabakkajökull the eastern most of studied outlets. This part of the glacier is open to precipitation from all south- and east- and north-easterly wind directions, and thus has high snow accumulation in winters when the paths of the North Atlantic lows is just east of Iceland. This is also the case for the eastern part of Brúarjökull.

Breiðamerkurjökull shows lowest variability. It is a maritime glacier with climate controlled by the stable sea temperature and humid air mass. The longest winter balance records seem to reveal periodic behavior, with peaks in ~1991_92 and 2002_03 and a low in ~1998. During the period of net mass loss since 1994_95, the northern outlets have had several years of close

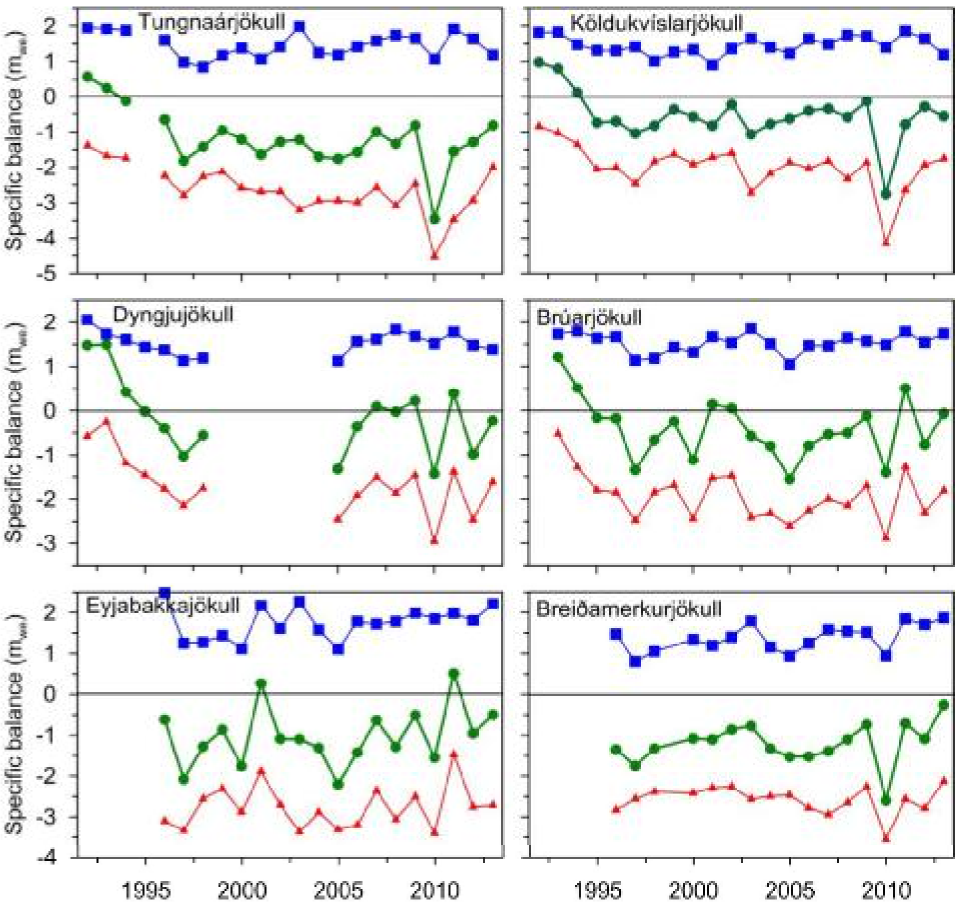

Figure 16. Specific mass balance record for Vatnajökull outlets 1991_92-2012_13.

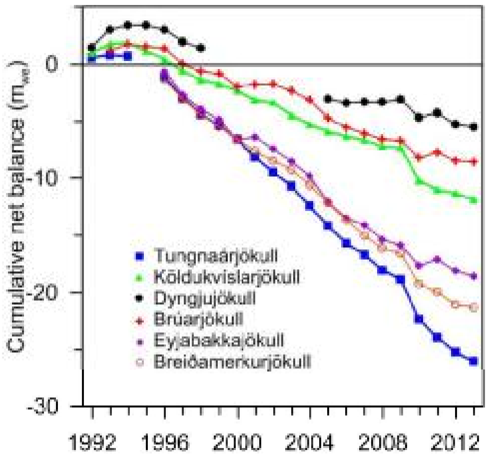

Figure 17. Cumulative specific mass balance for several of Vatnajökull outlets 1991_92 – 2012_13.

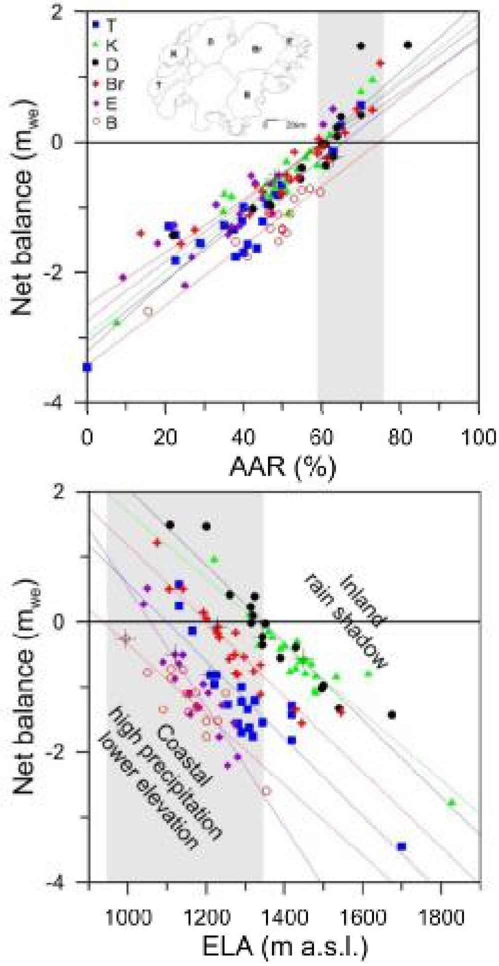

Figure 18. The relation between net annual balance (b_n) and accumulation area ratio (AAR)(upper) and b_n and equilibrium line altitude (ELA), for Vatnajökull outlets during the survey period. (This years points are marked with a black +).

to zero and positive mass balance.

The cumulative net balance curves for the outlets of Vatnajökull in Fig. 17 show that all outlets have been losing mass since 1994_95. The slope for mass loss is about 0.7 ma^{-1} for northern outlets but 1.5 ma^{-1} for the south and western outlets.

In Fig. 18 the relation of the annual net balance to the accumulation area ratio (AAR) and equilibrium line altitude (ELA) is shown for different outlets over the survey period. The b_n-AAR gradient is similar for all outlets, about 0.5 m_{we} for 10% change in AAR. The zero-balance AAR varies for different outlets from about 60-65%, similar for all outlets except for the southern outlet Breiðamerkurjökull.

Breiðamerkurjökull is far from equilibrium, the ablation area is too large. A large part of the glacier has carved 200-300 m through the former sediment bed, and the surface elevation has lowered accordingly. Breiðamerkurjökull is now retreating at a high rate.

Similarly the zero-balance ELA varies from about 1000-1100 m for the southern outlets to 1400 m for the NW outlets. The b_n-ELA slope is similar for all outlets -0.7 m_{we} per 100 m.

4. SURFACE VELOCITY MEASUREMENTS

The surface velocity of the glacier was calculated from DGPS (accuracy within 1 m), fast static (accuracy about 1 cm) and kinematic GPS (accuracy about 3 cm) positioning of the ablation stakes. All sites were surveyed in spring and autumn (most kinematic, some DGPS), and many also in June (kinematic), August (fast static) and October (kinematic). At a few sites stakes from previous years were found and resurveyed, making it possible to calculate surface velocity over a year or longer time span. The average summer surface velocity is shown on Figure 19.

The use of more accurate instruments and setup, allows estimation of vertical as well as horizontal velocities. Two 6 metre long 4 inch metal poles where set up in the accumulation zone of the western outlet Tungnaárjökull and one on east Brúarjökul to directly measure the vertical displacement. Small GPS units are also attached to the poles and run continuously. At sites close to the glacier edge very small horizontal movement is measured. This indicates that the glacier snouts are almost stagnant. In the centre areas of some of the outlets especially close to the equilibrium line, there is an increase in velocity during summer compared to winter. The summer velocity is of the order of two-fold the winter velocity. This suggests that basal sliding is increased in the melting season, and is of the same magnitude as the deformation velocity.

From previous velocity measurements, surging of outlets has been predicted. No signs of a starting surge are seen from this year's survey.

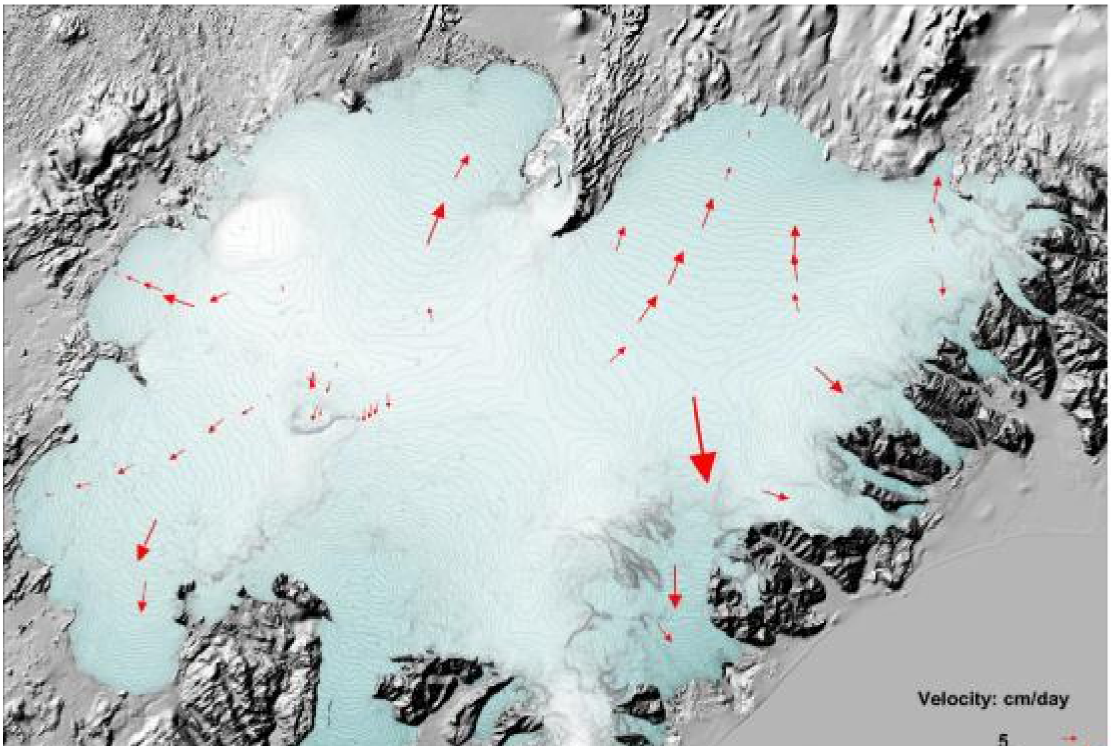

Figure 19. Average surface velocity at survey sites in 2012_13.

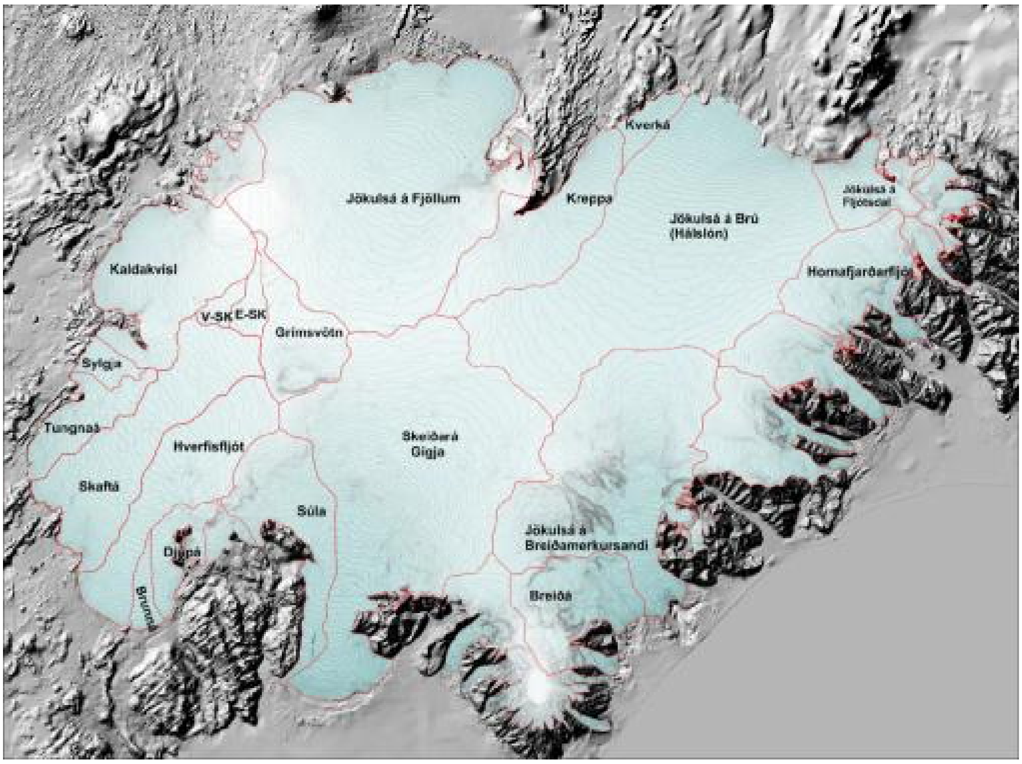

Figure 20. Water divides and drainage basins of selected rivers draining water from Vatnajökull.

5. Melt water runoff.

Water divides and drainage basins for rivers draining water from Vatnajökull have been defined from water pressure potential maps. The potential maps were produced from existing surface (year 2010) and bedrock digital elevation models.

Figure 20 shows the water divides and drainage areas for selected rivers draining melt water from Vatnajökull. The summer balance over the water basin is an estimate of meltwater contribution to rivers and groundwater storage. This estimate, however, does not include precipitation that falls as rain on the glacier, nor snow which falls and melts during the summer. The meltwater contribution can be compared with river runoff at stream flow gauges closest to the glacier. For this comparison, we define the glaciological year from the start of October to the end of September and the period draining meltwater from the glacier during the summer from June through September. It would be misleading to include May in the summer period because runoff from

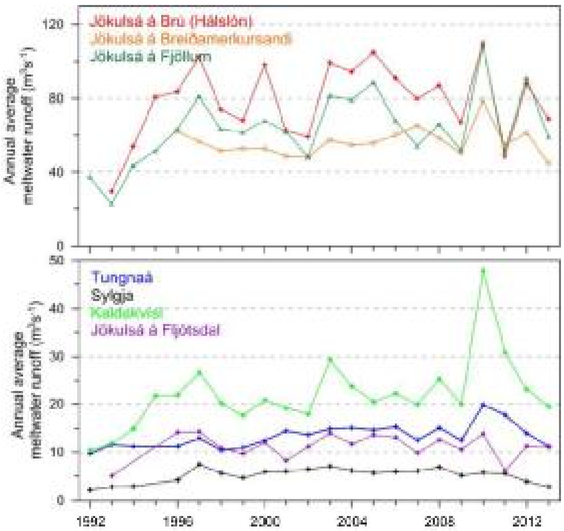

Figure 21. The temporal variation of average annual meltwater runoff to selcted river catchments.

Table I. Melt water drainage to selected rivers.

Water Catchment:	Area (km^2)	ΣQ_s ($10^6 m^3$)	Q_s ($m^3 s^{-1}$)	Q_a ($m^3 s^{-1}$)	q_s ($ls^{-1} km^{-2}$)
Vatnajökull	7968,0	14723,9	1396,8	466,9	58,6
Tungnaá	121,8	352,2	33,4	11,2	91,7
Sylgja	39,7	88,4	8,4	2,8	70,6
Kaldakvísl	367,9	610,6	57,9	19,4	52,6
Jokulsa a Fjöllum	1188,3	1858,1	176,3	58,9	49,6
Kreppa	291,2	409,9	38,9	13,0	44,6
Kverka	47,0	187,0	17,7	5,9	126,2
Jokulsa a Brú	1214,8	2175,9	206,4	69,0	56,8
Jökulsá á Fljótsdal	130,6	348,1	33,0	11,0	84,5
Jökulsá í Lóni	101,3	247,8	23,5	7,9	77,6
Hornafjarðarfljót	239,1	473,1	44,9	15,0	62,7
Jökulsá á Breiðamerkursandi	739,5	1404,5	133,2	44,5	60,2
Breiðá-Fjallsá	234,6	742,2	70,4	23,5	100,3
Skeiðará-Gígja	1165,2	1938,6	183,9	61,5	52,8
Súla	255,8	631,2	59,9	20,0	78,2
Brunná	35,8	128,7	12,2	4,1	114,0
Djúpá	83,7	225,7	21,4	7,2	85,5
Hverfisfljót	317,7	491,6	46,6	15,6	49,1
Skaftá	394,9	736,1	69,8	23,3	59,1
Grímsvötn	173,3	102,9	9,8	3,3	18,8
Eystri Skaftárketill	39,4	13,9	1,3	0,4	11,2
Vestari Skaftárketill	25,1	9,7	0,9	0,3	12,3
Hólmsá	164,9	342,9	32,5	10,9	65,9
Heinabergsvötn	229,6	502,0	47,6	15,9	69,3
Skjálfandafljót	71,9	83,9	8,0	2,7	37,0

ΣQ_s: total summer melt water; Q_s : average runoff (averaged over summer, 4 months, June – September)
Q_a : average runoff (averaged over a whole year); q_s : average runoff per km^2 (averaged over a whole year)

the glacier melt in May is delayed due to refreezing during elimination of the cold wave and because of the contribution of the spring melt from the highlands to the runoff. Some melting also occurs during winter, especially in the low snouts of the southern outlets.

Average melt water runoff to different rivers is given in Table I, and temporal variation of the average meltwater runoff in Fig. 21. The average specific runoff (q_s) differs from basin to basin from 11 to 126 $ls^{-1}km^{-2}$. This is mainly due to different elevation distributions, for example, the water drainage basins for Tungnaá and Kverká are within the ablation area, while that of Grímsvötn and Skaftárkatlar are high in the accumulation zone.

6. Conclusions

September 2012 was a stormy month, a northern snow blizzard in the second week delivered a thick snow layer N and NE Iceland, and some snow was accumulated on Vatnajökull, ablation came to an abrupt halt. Much of the winter was wet in west and south Iceland, snow accumulation on Vatnajökull dominantly in SE, E and NE wind. This resulted in exceptionally thick snow cover in the accumulation zone of E-Vatnajökull, whereas snow accumulation on the western half was less than average.

The summer was wet and cloudy in W and S Iceland, with a warm clear sky period late July and beginning of August in NE, E and SE Iceland. Early in June dust from the snow free highland north of Vatnajökull was blown over Brúarjökull and Dyngjujökull ablation zones and the accumulation zone of E-Brúarjökull, Eyjabakkajökull and the SE outlets. The resulting summer ablation was close to average on the northern outlets but much less than average on the W and SW outlets.

$B_{w:}$ of 13.133 km^3, B_s : -14.71 km^3 and B_n : -1.58 km^3 , AAR = 60%

(b_w= 1.65 m, b_s= -1.85, b_n= -0.20 m).

The winter balance was higher than average by 13% (over the observation period 1991_92-2011_12). The summer ablation was ~92% of the average over the survey period. The net balance was negative, the mass loss was only 27% of the average loss (-0.75 m) of the past 18 consecutive years of negative balance.

The glacial year of 2011_12 was the 19th in a row with negative mass balance for Vatnajökull (since 1994_95) contributing to a total loss of 13.7m_{we}, 0.75$m_{we}a^{-1}$ or an average surface lowering of 0.83ma^{-1}. This is equivalent to a total ice volume of ~122 km^3, or ~4% off the total ice mass.

Meltwater runoff to Tungnaá was ~83% of the average, 87% to Kaldakvísl, 92% to Jökulsá á Fjöllum, 87% to Jökulsá á Brú (Hálslón), 98% to Jökulsá í Fljótsdal and 78% to Jökulsá á Breiðamerkursandi (summer rain and snow that falls and melts during summer is not included).

Appendix A: Mass balance at measurement sites 2012_13.

b_w: specific winter balance, **b_s**: specific summer balance, **b_n**: specific net balance,
l_a: new snow in autumn (all in water equivalent).

Site	Position				Elevation	Date	Date	b_w	b_s	b_n	la
	Latitude		Longitude		(m a.s.l.)	in spring	in autumn	(mm)	(mm)	(mm)	(mm)
B09t	64	45,0426	16	5,4726	752,7	130506	131003	533	-5006	-4473	0
B10t	64	43,6866	16	6,7008	807,6	130506	131003	718	-4183	-3465	0
B11c	64	40,9410	16	10,4946	962,1	130506	131003	967	-3145	-2178	0
B12s	64	38,2752	16	14,1384	1077,3	130506	131003	1418	-2255	-837	70
B13s	64	34,5096	16	19,7514	1215,3	130506	131003	1507	-1612	-105	60
B14u	64	31,6386	16	24,6966	1314,3	130506	131003	1745	-1037	708	56
B15h	64	28,4826	16	30,0066	1398,6	130506	131003	1650	-996	654	70
B16u	64	24,1194	16	40,8522	1525,3	130508	131007	2140	-406	1734	140
B17s	64	36,7344	16	28,7982	1212,6	130506	131003	1335	-2325	-990	18
BR1g	64	5,5575	16	19,5031	112,9	130501	131008	-1330	-8046	-9376	0
BR2k	64	6,3977	16	22,5472	239,2	130131					
BR3p	64	8,5212	16	24,1212	404,9	130501		750			
BR4d	64	10,9345	16	20,2345	544,2	130501	131001	900	-4095	-3195	0
Br7q	64	22,1412	16	16,9440	1246,7	130508	131003	2680	-904	1776	35
B07r	64	25,7958	16	17,4588	1357,4	130508	131003	2430	-840	1590	63
BB0r	64	22,7166	16	5,0478	1519,6	130508	131002	2896	-826	2070	25
Brur	64	41,0016	15	55,2234	776,8	130506	131002	755	-5363	-4608	0
Budr	64	35,9892	15	59,8944	1135,7	130506	131002	1610	-1830	-220	7
gb2c	64	34,1064	16	0,0240	1200,6	130507	131002	2205	-1809	396	70
B18q	64	31,5822	16	0,1122	1312,1	130507	131002	2570	-1280	1290	88
B19q	64	27,9300	16	55,6500	1432,7	130507	131002	3720	-620	3100	63
BB0r	64	22,7166	16	5,0478	1519,6	130508	131002	2896	-826	2070	25
D05q	64	42,2208	16	54,6270	1201,3	130508	131004	1200	-2766	-1566	14
D07q	64	38,2830	16	59,2518	1369,1	130505	131004	1267	-1015	252	39
D09p	64	31,8006	17	0,5454	1579,9	130505	131004	1606	-502	1104	123
D12q	64	28,9842	17	0,1350	1646,1	130505	131003	1664	-350	1314	140
E01r	64	41,4528	15	33,4962	685,5	130507	131002	817	-5272	-4455	0
E02r	64	39,1350	15	35,9772	954,3	130507	131002	1522	-3646	-2124	14
E03r	64	36,6666	15	36,9144	1187,7	130507	131002	2920	-2020	900	123
E04r	64	34,9494	15	37,1016	1288,7	130507	131002	2930	-1598	1332	140
K01t	64	35,2674	17	52,3512	1011,3	130503	131004	542	-4790	-4248	0
K02u	64	34,8180	17	49,6842	1179,5	130503	131004	815	-2669	-1854	35
K03t	64	34,2474	17	46,3794	1297,5	130503	131004	803	-2107	-1304	70
K04u	64	33,2118	17	42,2496	1487,1	130503	131004	1129	-871	258	182
K05u	64	33,4500	17	35,4306	1680,2	130503	131004	1911	-351	1560	280
K06t	64	38,3544	17	31,3806	1967,6	130602	131004	1960	110	2070	410
K07p	64	29,1126	17	42,0144	1533,5	130503	131004	1192	-654	538	235
S01i	64	7,0080	17	49,9830	743,4	130504	131005	935	-3770	-2835	0
S02i	64	12,1554	17	48,9696	1009,5	130504	131005	860	-2561	-1701	11
S04m	64	16,2000	17	48,2214	1160,0	130504	131005	1147	-1477	-330	88
HAABm	64	20,9676	17	24,1188	1729,6	130604	131005	2390	-260	2130	280

T01nn	64	19,4838	18	8,2308	749,6	130501	131005	111	-5781	-5670	0
T02np	64	19,6014	18	3,9672	943,8	130501	131005	1125	-3222	-2097	0
T03np	64	20,2092	17	58,5990	1078,2	130501	131005	801	-2780	-1979	0
T04np	64	21,3414	17	51,5196	1221,9	130502	131005	1378	-1210	168	35
T05nn	64	22,2930	17	42,9918	1344,5	130502	131005	1627	-943	684	105
T06np	64	24,2760	17	36,5394	1464,0	130502	131005	2098	-538	1560	140
T07no	64	25,2894	17	31,1976	1562,5	130503	131005	1727	-431	1296	158
T08np	64	26,3130	17	27,7680	1636,1	130503	131004	1557	-471	1086	200
BORTHNb	64	25,1225	17	19,1470	1402,4	130601	131006	2230	-1162	1068	133
BORah	64	24,9480	17	20,1504	1400,6	130604	131004	1840	-1324	516	105
G02j	64	26,8518	17	17,7210	1560,1	130602	131004	1720	-700	1020	186
G03k	64	28,4388	17	16,3536	1654,5	130602	131004	1510	-466	1044	158
G04r	64	30,0264	17	15,0546	1684,1	130602	131004	1640	-422	1218	130
Go1q	64	33,9768	17	24,9450	1757,0	130602	131004	1690	-322	1368	179
Hof01k	64	32,3226	15	35,8416	1140,3	130507	131002	2512	-1198	1314	84
E04r	64	34,9494	15	37,1016	1288,7	130507	131002	2930	-1598	1332	140
Skf01d	64	17,9946	16	4,9962	1283,0	130508	131002	3658	-976	2682	81
Fl01d	64	25,9992	15	55,3080	1330,1	130508	131002	3270	-1104	2166	53

Appendix B: Balance distribution by elevation in 2012_13.

ΔS : area in elevation range, ∑ΔS: cumulative area above given elevation, b_w: specific winter balance, b_s: specific summer balance. b_n: specific winter balance, ΔB_w : winter balance at a given elevation range, $\sum\Delta B_w$: cumulative winter balance above given elevation, ΔB_s summer balance at a given elevation range, $\sum\Delta B_s$: cumulative summer balance above given elevation, ΔB_n: net annual balance in a given elevation range, $\sum B_n$: cumulative net annual balance above given elevation.

Vatnajökull

Elevation (m a.s.l.)			ΔS (km^2)	∑ΔS (km^2)	b_w (mm)	b_s (mm)	b_n (mm)	ΔB_w (10^6m^3)	$\sum\Delta B_w$ (10^6m^3)	ΔB_s (10^6m^3)	$\sum\Delta B_s$ (10^6m^3)	ΔB_n (10^6m^3)	$\sum B_n$ (10^6m^3)
2000	2050	2025	0,5	0,5	4417	28	4445	2,1	2	0,0	0	2,1	2
1950	2000	1975	16,3	16,8	2273	123	2396	37,1	39	2,0	2	39,1	41
1900	1950	1925	44,6	61,4	2186	57	2243	97,6	137	2,6	5	100,2	141
1850	1900	1875	35,8	97,2	2477	-72	2404	88,9	226	-2,6	2	86,3	228
1800	1850	1825	40,4	137,6	2752	-137	2614	111,3	337	-5,6	-4	105,8	334
1750	1800	1775	55,5	193,1	2356	-218	2138	131,3	468	-12,2	-16	119,1	453
1700	1750	1725	102,5	295,6	2078	-311	1766	213,6	682	-32,0	-48	181,5	634
1650	1700	1675	223,9	519,5	1922	-400	1521	430,8	1113	-89,8	-138	341,0	975
1600	1650	1625	355,2	874,7	1856	-424	1431	659,7	1773	-151,0	-289	508,7	1484
1550	1600	1575	355,7	1230,4	1884	-464	1419	670,4	2443	-165,2	-454	505,2	1989
1500	1550	1525	418,4	1648,8	1892	-522	1370	792,4	3235	-218,7	-673	573,6	2563
1450	1500	1475	450,3	2099,1	1945	-632	1313	876,7	4112	-285,0	-958	591,7	3154
1400	1450	1425	502,0	2601,1	2085	-778	1307	1047,9	5160	-391,2	-1349	656,7	3811
1350	1400	1375	537,1	3138,2	2153	-911	1242	1157,6	6318	-489,8	-1839	667,8	4479
1300	1350	1325	549,0	3687,2	2121	-1048	1073	1166,3	7484	-576,2	-2415	590,1	5069
1250	1300	1275	518,8	4206,0	2075	-1282	793	1078,7	8563	-666,4	-3081	412,3	5481
1200	1250	1225	463,8	4669,8	1890	-1542	347	878,6	9441	-717,1	-3798	161,5	5643
1150	1200	1175	411,2	5081,0	1735	-1836	-101	715,9	10157	-757,6	-4556	-41,7	5601
1100	1150	1125	367,9	5448,9	1608	-2101	-493	593,6	10751	-775,6	-5332	-182,0	5419
1050	1100	1075	331,3	5780,2	1460	-2388	-927	485,9	11237	-794,4	-6126	-308,6	5110
1000	1050	1025	306,2	6086,4	1326	-2713	-1386	408,1	11645	-834,5	-6961	-426,4	4684
950	1000	975	278,9	6365,3	1236	-3015	-1779	346,1	11991	-844,2	-7805	-498,1	4186
900	950	925	239,7	6605,0	1183	-3253	-2070	285,1	12276	-783,9	-8589	-498,8	3687
850	900	875	216,1	6821,1	1093	-3508	-2414	237,7	12513	-762,4	-9351	-524,7	3163
800	850	825	197,8	7018,9	998	-3755	-2756	199,2	12713	-748,9	-10100	-549,7	2613
750	800	775	170,7	7189,6	913	-4050	-3137	156,3	12869	-693,1	-10793	-536,8	2076
700	750	725	135,1	7324,7	933	-4078	-3145	126,5	12995	-553,0	-11346	-426,5	1649
650	700	675	101,6	7426,3	966	-4045	-3078	98,6	13094	-412,7	-11759	-314,1	1335
600	650	625	70,3	7496,6	1010	-3923	-2912	71,4	13165	-277,3	-12036	-205,9	1130
550	600	575	63,4	7560,0	942	-4054	-3112	60,3	13226	-259,2	-12295	-199,0	931
500	550	525	44,7	7604,7	786	-4291	-3504	35,6	13261	-194,0	-12489	-158,4	772
450	500	475	41,4	7646,1	624	-4700	-4076	26,1	13287	-196,5	-12686	-170,4	602
400	450	425	44,4	7690,5	420	-5165	-4744	18,9	13306	-231,9	-12918	-213,0	389
350	400	375	40,6	7731,1	93	-5649	-5555	3,9	13310	-232,8	-13150	-228,9	160
300	350	325	41,1	7772,2	-173	-6088	-6261	-7,2	13303	-253,5	-13404	-260,7	-101
250	300	275	40,4	7812,6	-476	-6580	-7056	-19,3	13284	-267,4	-13671	-286,7	-388
200	250	225	37,9	7850,5	-805	-7117	-7922	-30,8	13253	-271,7	-13943	-302,4	-690
150	200	175	31,6	7882,1	-1074	-7626	-8701	-34,2	13219	-243,0	-14186	-277,2	-967
100	150	125	32,4	7914,5	-1301	-8074	-9375	-42,8	13176	-265,4	-14451	-308,2	-1276
50	100	75	24,7	7939,2	-1512	-8309	-9821	-38,0	13138	-208,6	-14660	-246,6	-1522
0	50	25	6,1	7945,3	-1672	-8525	-10197	-10,6	13127	-54,2	-14714	-64,9	-1587

Tungnaárjökull

Elevation (m a.s.l.)			ΔS (km^2)	$\sum\Delta S$ (km^2)	b_w (mm)	b_s (mm)	b_n (mm)	ΔB_w (10^6m^3)	$\sum\Delta B_w$ (10^6m^3)	ΔB_s (10^6m^3)	$\sum\Delta B_s$ (10^6m^3)	ΔB_n (10^6m^3)	$\sum B_n$ (10^6m^3)
1650	1700	1675	2,4	2,4	1664	-437	1226	3,9	4	-1,0	-1	2,9	3
1600	1650	1625	13,2	15,6	1648	-427	1221	21,7	26	-5,6	-7	16,1	19
1550	1600	1575	15,3	30,9	1730	-421	1309	26,4	52	-6,4	-13	20,0	39
1500	1550	1525	15,3	46,2	1879	-453	1426	28,7	81	-6,9	-20	21,8	61
1450	1500	1475	18,5	64,7	2013	-513	1499	37,2	118	-9,5	-30	27,7	89
1400	1450	1425	23,3	88,0	1949	-635	1313	45,4	163	-14,8	-44	30,6	119
1350	1400	1375	21,7	109,7	1757	-808	948	38,1	202	-17,5	-62	20,5	140
1300	1350	1325	28,1	137,8	1589	-1003	585	44,6	246	-28,2	-90	16,4	156
1250	1300	1275	21,8	159,6	1465	-1187	277	32,0	278	-25,9	-116	6,1	162
1200	1250	1225	24,0	183,6	1316	-1420	-103	31,7	310	-34,1	-150	-2,5	160
1150	1200	1175	21,0	204,6	1126	-1699	-573	23,6	333	-35,6	-186	-12,0	148
1100	1150	1125	19,2	223,8	942	-2061	-1118	18,1	351	-39,7	-225	-21,5	126
1050	1100	1075	20,0	243,8	768	-2447	-1679	15,4	367	-49,0	-274	-33,6	93
1000	1050	1025	18,2	262,0	613	-2771	-2157	11,2	378	-50,4	-325	-39,3	53
950	1000	975	18,9	280,9	492	-3189	-2697	9,3	387	-60,2	-385	-51,0	2
900	950	925	15,2	296,1	397	-3721	-3323	6,0	393	-56,5	-441	-50,4	-48
850	900	875	15,1	311,2	333	-4309	-3975	5,0	398	-65,0	-506	-60,0	-108
800	850	825	14,1	325,3	249	-4941	-4692	3,5	402	-69,6	-576	-66,1	-174
750	800	775	10,3	335,6	178	-5479	-5300	1,8	404	-56,2	-632	-54,4	-229
700	750	725	7,1	342,7	142	-5846	-5703	1,0	405	-41,8	-674	-40,8	-269
650	700	675	1,6	344,3	150	-6029	-5878	0,3	405	-10,1	-684	-9,9	-279
600	650	625	0,0	344,3	136	-6124	-5987	0,0	405	-0,4	-685	-0,4	-280

Sylgjujökull

Elevation (m a.s.l.)			ΔS (km^2)	$\sum\Delta S$ (km^2)	b_w (mm)	b_s (mm)	b_n (mm)	ΔB_w (10^6m^3)	$\sum\Delta B_w$ (10^6m^3)	ΔB_s (10^6m^3)	$\sum\Delta B_s$ (10^6m^3)	ΔB_n (10^6m^3)	$\sum B_n$ (10^6m^3)
1600	1650	1625	2,0	2,0	1709	-403	1306	3,4	3	-0,8	-1	2,6	3
1550	1600	1575	6,8	8,8	1646	-436	1210	11,1	15	-2,9	-4	8,2	11
1500	1550	1525	18,9	27,7	1488	-493	994	28,1	43	-9,3	-13	18,8	30
1450	1500	1475	12,3	40,0	1595	-538	1056	19,6	62	-6,6	-20	13,0	43
1400	1450	1425	8,2	48,2	1661	-612	1049	13,7	76	-5,0	-25	8,6	51
1350	1400	1375	5,1	53,3	1630	-779	850	8,3	84	-4,0	-29	4,3	56
1300	1350	1325	5,3	58,6	1522	-1032	489	8,0	92	-5,4	-34	2,6	58
1250	1300	1275	10,4	69,0	1411	-1284	127	14,6	107	-13,3	-47	1,3	59
1200	1250	1225	12,6	81,6	1266	-1587	-320	15,9	123	-20,0	-67	-4,0	55
1150	1200	1175	14,4	96,0	1057	-1928	-870	15,2	138	-27,7	-95	-12,5	43
1100	1150	1125	13,2	109,2	843	-2321	-1478	11,1	149	-30,6	-126	-19,5	23
1050	1100	1075	13,4	122,6	677	-2760	-2083	9,1	158	-37,0	-163	-27,9	-5
1000	1050	1025	9,3	131,9	591	-3212	-2620	5,5	164	-29,8	-193	-24,3	-29
950	1000	975	3,1	135,0	564	-3467	-2903	1,7	165	-10,6	-203	-8,9	-38
900	950	925	1,6	136,6	491	-3738	-3246	0,8	166	-6,0	-209	-5,2	-43
850	900	875	0,2	136,8	445	-3967	-3521	0,0	166	-0,7	-210	-0,6	-44

Köldukvíslarjökul

Elevation (m a.s.l.)			ΔS (km^2)	∑ΔS (km^2)	b_w (mm)	b_s (mm)	b_n (mm)	$ΔB_w$ (10^6m^3)	$∑ΔB_w$ (10^6m^3)	$ΔB_s$ (10^6m^3)	$∑ΔB_s$ (10^6m^3)	$ΔB_n$ (10^6m^3)	$∑B_n$ (10^6m^3)
1950	2000	1975	3,6	3,6	2019	135	2155	7,3	7	0,5	1	7,7	8
1900	1950	1925	12,4	16,0	2046	60	2106	25,4	33	0,7	1	26,1	34
1850	1900	1875	5,9	21,9	2021	-34	1987	11,8	45	-0,2	1	11,6	46
1800	1850	1825	6,0	27,9	1988	-102	1886	11,9	56	-0,6	0	11,3	57
1750	1800	1775	10,5	38,4	2006	-155	1850	21,1	77	-1,6	-1	19,5	76
1700	1750	1725	17,9	56,3	1937	-266	1671	34,6	112	-4,8	-6	29,9	106
1650	1700	1675	15,6	71,9	1779	-415	1363	27,7	140	-6,5	-13	21,2	127
1600	1650	1625	13,8	85,7	1581	-529	1051	21,8	162	-7,3	-20	14,5	142
1550	1600	1575	19,2	104,9	1398	-612	786	26,9	189	-11,8	-32	15,1	157
1500	1550	1525	20,9	125,8	1201	-688	512	25,1	214	-14,4	-46	10,7	168
1450	1500	1475	19,3	145,1	1121	-899	222	21,7	235	-17,4	-63	4,3	172
1400	1450	1425	14,2	159,3	1048	-1210	-161	14,9	250	-17,2	-81	-2,3	170
1350	1400	1375	15,3	174,6	961	-1540	-578	14,7	265	-23,5	-104	-8,8	161
1300	1350	1325	17,5	192,1	886	-1927	-1041	15,5	280	-33,7	-138	-18,2	143
1250	1300	1275	18,0	210,1	847	-2256	-1409	15,3	296	-40,9	-179	-25,5	117
1200	1250	1225	18,3	228,4	815	-2552	-1737	14,9	311	-46,7	-225	-31,8	85
1150	1200	1175	16,4	244,8	772	-2987	-2215	12,7	323	-49,0	-274	-36,3	49
1100	1150	1125	14,9	259,7	713	-3613	-2899	10,7	334	-54,0	-328	-43,4	6
1050	1100	1075	13,1	272,8	651	-4236	-3585	8,6	343	-55,8	-384	-47,2	-42
1000	1050	1025	11,1	283,9	599	-4767	-4168	6,7	349	-53,0	-437	-46,4	-88
950	1000	975	10,5	294,4	558	-5229	-4671	5,9	355	-54,8	-492	-49,0	-137
900	950	925	5,6	300,0	529	-5611	-5082	3,0	358	-31,5	-523	-28,5	-165
850	900	875	0,5	300,5	512	-5978	-5466	0,3	358	-3,2	-527	-3,0	-168

Dyngjujökull

Elevation (m a.s.l.)			ΔS (km^2)	∑ΔS (km^2)	b_w (mm)	b_s (mm)	b_n (mm)	$ΔB_w$ (10^6m^3)	$∑ΔB_w$ (10^6m^3)	$ΔB_s$ (10^6m^3)	$∑ΔB_s$ (10^6m^3)	$ΔB_n$ (10^6m^3)	$∑B_n$ (10^6m^3)
1950	2000	1975	7,4	7,4	1972	140	2112	14,6	15	1,0	1	15,6	16
1900	1950	1925	23,2	30,6	2009	69	2078	46,5	61	1,6	3	48,1	64
1850	1900	1875	15,9	46,5	1954	-79	1874	31,1	92	-1,3	1	29,8	94
1800	1850	1825	9,7	56,2	1926	-177	1749	18,8	111	-1,7	0	17,0	111
1750	1800	1775	16,0	72,2	1916	-250	1666	30,6	142	-4,0	-4	26,6	137
1700	1750	1725	27,3	99,5	1883	-331	1551	51,3	193	-9,0	-13	42,3	180
1650	1700	1675	71,6	171,1	1820	-399	1421	130,3	323	-28,6	-42	101,7	281
1600	1650	1625	114,0	285,1	1719	-433	1285	196,1	519	-49,5	-92	146,6	428
1550	1600	1575	94,7	379,8	1657	-496	1160	157,0	676	-47,0	-139	109,9	538
1500	1550	1525	89,7	469,5	1562	-593	968	140,0	816	-53,2	-192	86,9	625
1450	1500	1475	75,1	544,6	1452	-731	720	109,0	926	-54,9	-247	54,1	679
1400	1450	1425	61,4	606,0	1373	-824	549	84,3	1010	-50,6	-297	33,7	713
1350	1400	1375	49,4	655,4	1305	-989	315	64,5	1074	-48,9	-346	15,6	728
1300	1350	1325	37,9	693,3	1255	-1294	-39	47,6	1122	-49,1	-395	-1,5	727
1250	1300	1275	41,3	734,6	1218	-1715	-496	50,4	1172	-70,9	-466	-20,5	706
1200	1250	1225	48,8	783,4	1184	-2291	-1107	57,9	1230	-112,0	-578	-54,1	652
1150	1200	1175	48,2	831,6	1134	-2903	-1768	54,7	1285	-140,1	-718	-85,3	567
1100	1150	1125	44,0	875,6	1069	-3286	-2217	47,1	1332	-144,7	-863	-97,6	469
1050	1100	1075	33,1	908,7	1000	-3619	-2618	33,2	1365	-120,0	-983	-86,8	382
1000	1050	1025	35,5	944,2	903	-3950	-3046	32,2	1397	-141,0	-1124	-108,7	273
950	1000	975	30,8	975,0	803	-4320	-3517	24,8	1422	-133,2	-1257	-108,4	165
900	950	925	25,6	1000,6	702	-4687	-3984	18,1	1440	-121,0	-1378	-102,9	62
850	900	875	24,9	1025,5	592	-5056	-4464	15,1	1455	-128,4	-1507	-113,3	-51
800	850	825	19,7	1045,2	472	-5382	-4910	9,6	1465	-108,9	-1616	-99,4	-151
750	800	775	15,2	1060,4	309	-5754	-5444	4,7	1470	-87,2	-1703	-82,5	-233
700	750	725	1,7	1062,1	212	-5959	-5746	0,4	1470	-10,4	-1713	-10,0	-243

Brúarjökull

Elevation (m a.s.l.)			ΔS (km^2)	$\sum\Delta S$ (km^2)	b_w (mm)	b_s (mm)	b_n (mm)	ΔB_w ($10^6 m^3$)	$\sum\Delta B_w$ ($10^6 m^3$)	ΔB_s ($10^6 m^3$)	$\sum\Delta B_s$ ($10^6 m^3$)	ΔB_n ($10^6 m^3$)	$\sum B_n$ ($10^6 m^3$)
1850	1900	1875	0,8	0,8	1912	-253	1659	1,7	2	-0,2	0	1,4	1
1800	1850	1825	4,2	5,0	1911	-166	1745	7,9	10	-0,7	-1	7,2	9
1750	1800	1775	3,0	8,0	1883	-223	1660	5,6	15	-0,7	-2	4,9	14
1700	1750	1725	3,7	11,7	1848	-305	1543	6,9	22	-1,1	-3	5,8	19
1650	1700	1675	5,3	17,0	1823	-339	1483	9,6	32	-1,8	-5	7,8	27
1600	1650	1625	44,4	61,4	1773	-366	1406	78,8	111	-16,3	-21	62,5	90
1550	1600	1575	47,6	109,0	1864	-382	1481	88,8	199	-18,2	-39	70,6	160
1500	1550	1525	69,8	178,8	1971	-449	1521	137,7	337	-31,4	-70	106,3	267
1450	1500	1475	73,9	252,7	1870	-592	1277	138,3	475	-43,8	-114	94,5	361
1400	1450	1425	108,1	360,8	2112	-818	1294	228,5	704	-88,5	-203	140,0	501
1350	1400	1375	148,2	509,0	2244	-949	1294	332,8	1037	-140,8	-344	192,0	693
1300	1350	1325	151,3	660,3	2217	-1074	1143	335,7	1372	-162,6	-506	173,0	866
1250	1300	1275	144,8	805,1	2160	-1353	806	312,9	1685	-196,1	-702	116,8	983
1200	1250	1225	121,8	926,9	1970	-1650	320	240,1	1925	-201,0	-903	39,1	1022
1150	1200	1175	105,8	1032,7	1752	-1921	-168	185,5	2111	-203,3	-1107	-17,9	1004
1100	1150	1125	86,8	1119,5	1563	-2188	-625	135,7	2246	-190,0	-1297	-54,3	950
1050	1100	1075	73,3	1192,8	1417	-2452	-1034	104,0	2350	-179,9	-1476	-75,9	874
1000	1050	1025	65,6	1258,4	1231	-2828	-1596	80,8	2431	-185,7	-1662	-104,8	769
950	1000	975	59,4	1317,8	1055	-3239	-2183	62,7	2494	-192,3	-1854	-129,6	639
900	950	925	48,9	1366,7	932	-3623	-2690	45,6	2539	-177,2	-2032	-131,6	508
850	900	875	44,9	1411,6	840	-3924	-3084	37,7	2577	-176,1	-2208	-138,4	370
800	850	825	41,4	1453,0	760	-4229	-3469	31,5	2609	-175,0	-2383	-143,5	226
750	800	775	36,1	1489,1	666	-4800	-4134	24,1	2633	-173,3	-2556	-149,3	77
700	750	725	23,8	1512,9	578	-5314	-4735	13,7	2646	-126,2	-2682	-112,5	-36
650	700	675	12,8	1525,7	424	-5676	-5252	5,4	2652	-72,5	-2755	-67,1	-103
600	650	625	0,3	1526,0	354	-5971	-5617	0,1	2652	-2,0	-2757	-1,9	-105

Eyjabakkajökull

Elevation (m a.s.l.)			ΔS (km^2)	$\sum\Delta S$ (km^2)	b_w (mm)	b_s (mm)	b_n (mm)	ΔB_w ($10^6 m^3$)	$\sum\Delta B_w$ ($10^6 m^3$)	ΔB_s ($10^6 m^3$)	$\sum\Delta B_s$ ($10^6 m^3$)	ΔB_n ($10^6 m^3$)	$\sum B_n$ ($10^6 m^3$)
1550	1600	1575	0,0	0,0	3395	-1080	2314	0,0	0	0,0	0	0,0	0
1500	1550	1525	0,0	0,0	3443	-1048	2395	0,3	0	0,0	0	0,2	0
1450	1500	1475	1,0	1,0	3380	-1070	2310	3,3	4	-1,0	-1	2,2	3
1400	1450	1425	1,8	2,8	3324	-1118	2205	6,1	10	-2,1	-3	4,1	7
1350	1400	1375	2,5	5,3	3200	-1232	1967	8,1	18	-3,1	-6	5,0	12
1300	1350	1325	3,9	9,2	3063	-1372	1691	12,0	30	-5,4	-12	6,6	18
1250	1300	1275	13,4	22,6	2883	-1621	1262	38,5	68	-21,7	-33	16,9	35
1200	1250	1225	13,3	35,9	2795	-1853	941	37,2	106	-24,7	-58	12,5	48
1150	1200	1175	14,7	50,6	2628	-2137	491	38,6	144	-31,4	-89	7,2	55
1100	1150	1125	12,3	62,9	2361	-2459	-97	29,0	173	-30,2	-120	-1,2	54
1050	1100	1075	10,6	73,5	2034	-2837	-802	21,5	195	-30,0	-150	-8,5	45
1000	1050	1025	10,1	83,6	1744	-3217	-1472	17,7	212	-32,6	-182	-14,9	30
950	1000	975	7,7	91,3	1522	-3609	-2086	11,8	224	-27,9	-210	-16,2	14
900	950	925	5,2	96,5	1351	-4013	-2661	7,0	231	-20,8	-231	-13,8	0
850	900	875	3,9	100,4	1270	-4291	-3020	5,0	236	-16,7	-248	-11,8	-12
800	850	825	3,2	103,6	1208	-4478	-3270	3,8	240	-14,2	-262	-10,3	-22
750	800	775	3,4	107,0	1097	-4720	-3622	3,7	244	-15,9	-278	-12,2	-34
700	750	725	3,3	110,3	920	-5070	-4150	3,0	247	-16,7	-295	-13,7	-48
650	700	675	1,7	112,0	809	-5420	-4610	1,4	248	-9,2	-304	-7,8	-56

Hoffellsjökull

Elevation (m a.s.l.)			ΔS (km^2)	$\sum\Delta S$ (km^2)	b_w (mm)	b_s (mm)	b_n (mm)	ΔB_w (10^6m^3)	$\sum\Delta B_w$ (10^6m^3)	ΔB_s (10^6m^3)	$\sum\Delta B_s$ (10^6m^3)	ΔB_n (10^6m^3)	$\sum B_n$ (10^6m^3)
1450	1500	1475	0,9	0,9	3394	-1049	2344	3,1	3	-1,0	-1	2,2	2
1400	1450	1425	6,7	7,6	3383	-933	2449	22,7	26	-6,3	-7	16,4	19
1350	1400	1375	10,0	17,6	3265	-1006	2259	32,6	58	-10,0	-17	22,5	41
1300	1350	1325	15,4	33,0	3083	-1102	1980	47,4	106	-16,9	-34	30,4	72
1250	1300	1275	33,6	66,6	2860	-1256	1604	96,0	202	-42,1	-76	53,8	125
1200	1250	1225	26,8	93,4	2708	-1150	1558	72,6	274	-30,8	-107	41,8	167
1150	1200	1175	18,2	111,6	2568	-1138	1430	46,8	321	-20,7	-128	26,0	193
1100	1150	1125	17,5	129,1	2427	-1276	1150	42,5	364	-22,3	-150	20,1	213
1050	1100	1075	13,6	142,7	2235	-1514	720	30,3	394	-20,6	-171	9,8	223
1000	1050	1025	10,0	152,7	2072	-1769	302	20,7	415	-17,7	-189	3,0	226
950	1000	975	9,0	161,7	1960	-2066	-105	17,7	432	-18,6	-207	-0,9	225
900	950	925	6,4	168,1	1903	-2366	-462	12,3	445	-15,2	-222	-3,0	222
850	900	875	4,3	172,4	1843	-2641	-797	8,0	453	-11,4	-234	-3,5	219
800	850	825	3,5	175,9	1792	-2793	-1001	6,4	459	-10,0	-244	-3,6	215
750	800	775	3,8	179,7	1722	-3005	-1282	6,7	466	-11,7	-256	-5,0	210
700	750	725	3,8	183,5	1587	-3228	-1641	6,1	472	-12,4	-268	-6,3	204
650	700	675	3,4	186,9	1387	-3484	-2097	4,7	476	-11,7	-280	-7,0	197
600	650	625	2,5	189,4	1125	-3733	-2608	2,8	479	-9,2	-289	-6,4	190
550	600	575	1,8	191,2	889	-3975	-3085	1,6	481	-7,2	-296	-5,6	185
500	550	525	1,5	192,7	701	-4285	-3584	1,0	482	-6,3	-302	-5,3	179
450	500	475	0,9	193,6	527	-4712	-4185	0,5	482	-4,4	-307	-3,9	176
400	450	425	0,9	194,5	341	-5226	-4884	0,3	483	-5,0	-312	-4,6	171
350	400	375	0,6	195,1	195	-5749	-5553	0,1	483	-3,4	-315	-3,3	168
300	350	325	0,9	196,0	75	-6169	-6094	0,0	483	-5,6	-321	-5,5	162
250	300	275	2,1	198,1	-286	-6641	-6928	-0,6	482	-14,4	-335	-15,0	147
200	250	225	3,3	201,4	-738	-7066	-7804	-2,4	480	-23,1	-358	-25,5	122
150	200	175	2,6	204,0	-1137	-7570	-8708	-3,0	477	-19,7	-378	-22,6	99
100	150	125	2,1	206,1	-1384	-8009	-9394	-2,9	474	-17,1	-395	-20,0	79
50	100	75	2,8	208,9	-1608	-8237	-9846	-4,4	469	-22,7	-418	-27,2	52
0	50	25	0,5	209,4	-1678	-8353	-10032	-0,8	469	-4,1	-422	-4,9	47

Breiðamerkurjökull

Elevation (m a.s.l.)			ΔS (km^2)	$\sum\Delta S$ (km^2)	b_w (mm)	b_s (mm)	b_n (mm)	ΔB_w ($10^6 m^3$)	$\sum\Delta B_w$ ($10^6 m^3$)	ΔB_s ($10^6 m^3$)	$\sum\Delta B_s$ ($10^6 m^3$)	ΔB_n ($10^6 m^3$)	$\sum B_n$ ($10^6 m^3$)
1900	1950	1925	0,0	0,0	4941	-16	4924	0,2	0	0,0	0	0,2	0
1850	1900	1875	0,4	0,4	4917	-52	4864	1,8	2	0,0	0	1,8	2
1800	1850	1825	0,4	0,8	4821	-117	4703	2,2	4	0,0	0	2,1	4
1750	1800	1775	0,8	1,6	4564	-190	4373	3,7	8	-0,2	0	3,6	8
1700	1750	1725	2,5	4,1	3499	-299	3200	8,6	17	-0,7	-1	7,9	16
1650	1700	1675	5,8	9,9	2769	-343	2425	16,0	33	-2,0	-3	14,0	30
1600	1650	1625	15,8	25,7	2541	-369	2172	40,2	73	-5,8	-9	34,3	64
1550	1600	1575	25,7	51,4	2405	-400	2004	61,9	135	-10,3	-19	51,6	115
1500	1550	1525	32,2	83,6	2354	-494	1860	75,7	210	-15,9	-35	59,8	175
1450	1500	1475	44,3	127,9	2458	-628	1830	108,8	319	-27,8	-63	81,0	256
1400	1450	1425	58,3	186,2	2426	-744	1681	141,6	461	-43,5	-106	98,1	354
1350	1400	1375	88,7	274,9	2488	-839	1648	220,7	681	-74,5	-181	146,2	501
1300	1350	1325	96,9	371,8	2509	-866	1642	243,2	925	-84,0	-265	159,2	660
1250	1300	1275	59,4	431,2	2512	-922	1589	149,3	1074	-54,8	-320	94,5	754
1200	1250	1225	39,7	470,9	2474	-1009	1465	98,2	1172	-40,1	-360	58,1	812
1150	1200	1175	32,6	503,5	2415	-1173	1241	78,8	1251	-38,3	-398	40,5	853
1100	1150	1125	27,7	531,2	2345	-1407	937	65,0	1316	-39,0	-437	26,0	879
1050	1100	1075	24,1	555,3	2247	-1653	593	54,1	1370	-39,8	-477	14,3	893
1000	1050	1025	22,1	577,4	2145	-1869	276	47,5	1417	-41,4	-518	6,1	899
950	1000	975	24,5	601,9	2009	-2130	-120	49,3	1467	-52,2	-570	-3,0	896
900	950	925	27,3	629,2	1914	-2355	-440	52,4	1519	-64,5	-635	-12,1	884
850	900	875	26,2	655,4	1736	-2640	-903	45,5	1565	-69,2	-704	-23,7	861
800	850	825	26,0	681,4	1492	-2845	-1353	38,9	1604	-74,2	-778	-35,3	825
750	800	775	25,3	706,7	1278	-3066	-1787	32,3	1636	-77,5	-856	-45,2	780
700	750	725	23,9	730,6	1204	-3298	-2093	28,8	1665	-78,9	-935	-50,1	730
650	700	675	30,8	761,4	1170	-3486	-2316	36,1	1701	-107,5	-1042	-71,4	659
600	650	625	26,2	787,6	1114	-3700	-2586	29,2	1730	-97,0	-1139	-67,8	591
550	600	575	26,8	814,4	1029	-3910	-2880	27,8	1758	-105,5	-1245	-77,7	513
500	550	525	15,6	830,0	984	-4194	-3209	15,5	1773	-66,0	-1311	-50,5	463
450	500	475	16,2	846,2	857	-4683	-3825	13,9	1787	-76,1	-1387	-62,2	401
400	450	425	15,8	862,0	708	-5143	-4435	11,2	1798	-81,7	-1468	-70,4	330
350	400	375	12,9	874,9	424	-5611	-5187	5,5	1804	-73,2	-1542	-67,7	262
300	350	325	12,9	887,8	20	-6062	-6042	0,3	1804	-79,2	-1621	-78,9	184
250	300	275	12,0	899,8	-453	-6640	-7093	-5,5	1799	-80,0	-1701	-85,5	98
200	250	225	11,5	911,3	-906	-7317	-8223	-10,4	1788	-84,1	-1785	-94,5	4
150	200	175	8,5	919,8	-1240	-7856	-9096	-10,6	1778	-67,4	-1852	-78,1	-75
100	150	125	7,9	927,7	-1446	-8214	-9660	-11,4	1766	-64,6	-1917	-76,0	-151
50	100	75	6,0	933,7	-1564	-8462	-10027	-9,5	1757	-51,4	-1968	-60,9	-211
0	50	25	2,9	936,6	-1632	-8595	-10227	-5,0	1752	-26,3	-1995	-31,3	-243

Síðujökull

Elevation (m a.s.l.)			ΔS (km^2)	∑ΔS (km^2)	b_w (mm)	b_s (mm)	b_n (mm)	$ΔB_w$ (10^6m^3)	$∑ΔB_w$ (10^6m^3)	$ΔB_s$ (10^6m^3)	$∑ΔB_s$ (10^6m^3)	$ΔB_n$ (10^6m^3)	$∑B_n$ (10^6m^3)
1700	1750	1725	0,7	0,7	2124	-308	1815	1,6	2	-0,2	0	1,4	1
1650	1700	1675	5,2	5,9	2050	-373	1676	10,6	12	-1,9	-2	8,6	10
1600	1650	1625	11,1	17,0	1930	-401	1529	21,5	34	-4,5	-7	17,0	27
1550	1600	1575	10,1	27,1	1937	-405	1531	19,6	53	-4,1	-11	15,5	43
1500	1550	1525	20,1	47,2	1987	-441	1546	40,0	93	-8,9	-20	31,1	74
1450	1500	1475	40,1	87,3	2016	-513	1502	80,9	174	-20,6	-40	60,3	134
1400	1450	1425	26,9	114,2	1950	-632	1317	52,4	227	-17,0	-57	35,4	169
1350	1400	1375	21,3	135,5	1787	-812	975	38,1	265	-17,3	-75	20,8	190
1300	1350	1325	17,4	152,9	1625	-971	654	28,3	293	-16,9	-92	11,4	202
1250	1300	1275	16,6	169,5	1496	-1129	367	24,8	318	-18,7	-110	6,1	208
1200	1250	1225	21,2	190,7	1349	-1267	81	28,6	346	-26,8	-137	1,7	209
1150	1200	1175	18,1	208,8	1183	-1451	-268	21,4	368	-26,3	-163	-4,9	205
1100	1150	1125	17,0	225,8	1070	-1736	-666	18,2	386	-29,6	-193	-11,4	193
1050	1100	1075	18,0	243,8	969	-2107	-1137	17,4	403	-37,9	-231	-20,5	173
1000	1050	1025	21,8	265,6	892	-2501	-1609	19,4	423	-54,5	-285	-35,0	138
950	1000	975	21,8	287,4	857	-2867	-2009	18,7	442	-62,6	-348	-43,9	94
900	950	925	22,1	309,5	853	-3155	-2302	18,9	461	-69,8	-418	-50,9	43
850	900	875	20,9	330,4	852	-3382	-2530	17,8	478	-70,6	-488	-52,8	-10
800	850	825	25,0	355,4	846	-3573	-2727	21,2	499	-89,3	-578	-68,2	-78
750	800	775	25,5	380,9	828	-3729	-2900	21,1	521	-95,1	-673	-73,9	-152
700	750	725	26,0	406,9	770	-3899	-3128	20,0	541	-101,3	-774	-81,3	-233
650	700	675	15,8	422,7	688	-4123	-3434	10,9	551	-65,3	-839	-54,4	-288
600	650	625	7,4	430,1	636	-4309	-3673	4,7	556	-31,9	-871	-27,2	-315
550	600	575	0,2	430,3	665	-4434	-3768	0,1	556	-0,9	-872	-0,8	-316

Skaftárjökull

Elevation (m a.s.l.)			ΔS (km^2)	∑ΔS (km^2)	b_w (mm)	b_s (mm)	b_n (mm)	$ΔB_w$ (10^6m^3)	$∑ΔB_w$ (10^6m^3)	$ΔB_s$ (10^6m^3)	$∑ΔB_s$ (10^6m^3)	$ΔB_n$ (10^6m^3)	$∑B_n$ (10^6m^3)
1350	1400	1375	2,4	2,4	1734	-860	874	4,2	4	-2,1	-2	2,1	2
1300	1350	1325	5,5	7,9	1608	-1013	594	8,8	13	-5,5	-8	3,2	5
1250	1300	1275	4,5	12,4	1462	-1195	267	6,6	20	-5,4	-13	1,2	7
1200	1250	1225	6,5	18,9	1286	-1359	-72	8,3	28	-8,8	-22	-0,5	6
1150	1200	1175	9,3	28,2	1124	-1575	-450	10,4	38	-14,6	-36	-4,2	2
1100	1150	1125	12,3	40,5	982	-1887	-905	12,0	50	-23,1	-60	-11,1	-9
1050	1100	1075	14,2	54,7	866	-2240	-1373	12,3	63	-31,7	-91	-19,5	-29
1000	1050	1025	12,1	66,8	787	-2611	-1824	9,5	72	-31,6	-123	-22,1	-51
950	1000	975	7,6	74,4	729	-2978	-2248	5,5	78	-22,6	-146	-17,1	-68
900	950	925	5,3	79,7	675	-3312	-2636	3,6	81	-17,6	-163	-14,0	-82
850	900	875	5,6	85,3	620	-3735	-3114	3,4	85	-20,7	-184	-17,3	-99
800	850	825	5,7	91,0	551	-4278	-3727	3,2	88	-25,0	-209	-21,8	-121
750	800	775	5,1	96,1	513	-4638	-4124	2,6	91	-23,8	-233	-21,2	-142
700	750	725	3,6	99,7	470	-5033	-4563	1,7	92	-17,9	-251	-16,2	-158
650	700	675	2,8	102,5	479	-5208	-4728	1,4	94	-14,7	-265	-13,3	-172
600	650	625	0,8	103,3	427	-5425	-4998	0,3	94	-4,2	-269	-3,8	-176

Vestari Skaftárketill

Elevation (m a.s.l.)			ΔS (km^2)	∑ΔS (km^2)	b_w (mm)	b_s (mm)	b_n (mm)	$ΔB_w$ (10^6m^3)	∑$ΔB_w$ (10^6m^3)	$ΔB_s$ (10^6m^3)	∑$ΔB_s$ (10^6m^3)	$ΔB_n$ (10^6m^3)	∑B_n (10^6m^3)
1900	1950	1925	0,7	0,7	2069	16	2086	1,4	1	0,0	0	1,4	1
1850	1900	1875	0,6	1,3	2059	-22	2037	1,2	3	0,0	0	1,2	3
1800	1850	1825	0,7	2,0	2054	-73	1980	1,5	4	0,0	0	1,5	4
1750	1800	1775	2,7	4,7	2030	-198	1831	5,5	10	-0,5	-1	4,9	9
1700	1750	1725	5,9	10,6	1953	-275	1677	11,5	21	-1,6	-2	9,8	19
1650	1700	1675	6,7	17,3	1800	-359	1440	12,0	33	-2,4	-5	9,6	28
1600	1650	1625	7,4	24,7	1689	-406	1282	12,5	46	-3,0	-8	9,5	38
1550	1600	1575	5,2	29,9	1590	-435	1154	8,2	54	-2,2	-10	6,0	44
1500	1550	1525	1,5	31,4	1568	-441	1127	2,3	56	-0,6	-11	1,7	46

Eystri Skaftárketill

Elevation (m a.s.l.)			ΔS (km^2)	∑ΔS (km^2)	b_w (mm)	b_s (mm)	b_n (mm)	$ΔB_w$ (10^6m^3)	∑$ΔB_w$ (10^6m^3)	$ΔB_s$ (10^6m^3)	∑$ΔB_s$ (10^6m^3)	$ΔB_n$ (10^6m^3)	∑B_n (10^6m^3)
1750	1800	1775	1,1	1,1	2010	-254	1756	2,2	2	-0,3	0	1,9	2
1700	1750	1725	11,1	12,2	1918	-320	1597	21,4	24	-3,6	-4	17,8	20
1650	1700	1675	16,2	28,4	1798	-375	1423	29,1	53	-6,1	-10	23,0	43
1600	1650	1625	9,2	37,6	1738	-386	1352	16,1	69	-3,6	-14	12,5	55
1550	1600	1575	2,2	39,8	1727	-388	1339	3,8	73	-0,9	-14	3,0	58

Gjálp

Elevation (m a.s.l.)			ΔS (km^2)	∑ΔS (km^2)	b_w (mm)	b_s (mm)	b_n (mm)	$ΔB_w$ (10^6m^3)	∑$ΔB_w$ (10^6m^3)	$ΔB_s$ (10^6m^3)	∑$ΔB_s$ (10^6m^3)	$ΔB_n$ (10^6m^3)	∑B_n (10^6m^3)
1900	1950	1925	0,5	0,5	2062	23	2086	1,1	1	0,0	0	1,1	1
1850	1900	1875	0,6	1,1	2047	-41	2006	1,3	2	0,0	0	1,2	2
1800	1850	1825	1,2	2,3	2039	-122	1916	2,4	5	-0,1	0	2,2	5
1750	1800	1775	4,5	6,8	2004	-263	1740	9,1	14	-1,2	-1	7,9	13
1700	1750	1725	15,9	22,7	1919	-354	1564	30,6	45	-5,7	-7	24,9	38
1650	1700	1675	16,5	39,2	1877	-389	1487	31,0	76	-6,4	-13	24,6	62
1600	1650	1625	0,0	39,2	1874	-387	1487	0,0	76	0,0	-14	0,0	62

Grímsvötn

Elevation (m a.s.l.)			ΔS (km^2)	∑ΔS (km^2)	b_w (mm)	b_s (mm)	b_n (mm)	$ΔB_w$ (10^6m^3)	∑$ΔB_w$ (10^6m^3)	$ΔB_s$ (10^6m^3)	∑$ΔB_s$ (10^6m^3)	$ΔB_n$ (10^6m^3)	∑B_n (10^6m^3)
1700	1750	1725	0,8	0,8	1879	-400	1479	1,5	2	-0,3	0	1,2	1
1650	1700	1675	40,8	41,6	1867	-449	1417	76,3	78	-18,4	-19	57,9	59
1600	1650	1625	30,6	72,2	1869	-551	1318	57,3	135	-16,9	-36	40,4	100
1550	1600	1575	18,6	90,8	1924	-646	1277	35,9	171	-12,1	-48	23,8	123
1500	1550	1525	16,9	107,7	1959	-751	1207	33,0	204	-12,7	-60	20,4	144
1450	1500	1475	11,6	119,3	1983	-951	1031	23,0	227	-11,0	-71	12,0	156
1400	1450	1425	15,1	134,4	2017	-1218	798	30,4	257	-18,4	-90	12,0	168
1350	1400	1375	0,6	135,0	2025	-1018	1006	1,3	259	-0,7	-90	0,7	168

Appendix C: Coordinates at velocity measurement stakes.

Position of velocity measurement stakes determined by GPS sub-metre differential (I), fast static (FS) and kinematic (K).
(Accuracy of horizontal position 0.5 – 1.0 m, and vertical accuracy 1-2 m for DGPS, about 1cm for fast static, and 3 cm for kinematic).
The station Hofn in Höfn í Hornafirði is used as a stationary reference for all measurements, ÍSN93 datum, h_l is elevation above ellipsoid, dL antenna height, N estimated difference between ellipsoid and sea-level, H elevation in metres above sea level (H= h_l+N+dL). X and Y are ÍSN93 Lambert conformal conic projected coordinates. M is a quality marker.

Site	time	Date	#	Calender Day	Year	Latitude		Longitude		h_l (m a. e.)	dL (m)	N (m)	H (m a. s. l.)	X	Y	M
B07s	17,100	8	5	128	2013	64	25,79580	16	17,45880	1424,5	0,0	-67,1	1357,4	630472,14	439244,00	K
B07s	10,784	3	10	276	2013	64	25,79520	16	17,45820	1420,9	0,0	-67,1	1353,8	630472,66	439242,85	K
B09t	17,604	6	5	126	2013	64	45,04260	16	5,47260	819,4	0,0	-66,7	752,7	638442,06	475394,50	FS
B09t	16,077	3	10	276	2013	64	45,04260	16	5,47200	813,2	0,0	-66,7	746,6	638442,26	475394,67	K
B10s	15,915	6	5	126	2013	64	43,68840	16	6,70020	875,4	0,0	-66,7	807,7	637583,84	472835,69	K
B10t	16,644	6	5	126	2013	64	43,68660	16	6,70080	874,3	0,0	-66,7	807,6	637583,19	472832,37	K
B10t	15,828	3	10	276	2013	64	43,68660	16	6,70020	868,8	0,0	-66,7	802,1	637583,67	472832,34	K
B11c	15,253	6	5	126	2013	64	40,94100	16	10,49460	1028,9	0,0	-66,8	962,1	634801,35	467600,06	K
B11c	14,994	3	10	276	2013	64	40,94400	16	10,49100	1024,4	0,0	-66,8	957,6	634803,96	467606,68	K
B12s	14,316	6	5	126	2013	64	38,27520	16	14,13840	1144,2	0,0	-66,9	1077,3	632122,18	462524,46	K
B12s	14,375	3	10	276	2013	64	38,28300	16	14,13060	1140,3	0,0	-66,9	1073,4	632127,38	462539,20	K
B13s	10,629	6	5	126	2013	64	34,50960	16	19,75140	1282,3	0,0	-67,0	1215,3	627948,77	455342,02	K
B13s	11,854	3	10	276	2013	64	34,51860	16	19,74180	1278,3	0,0	-67,0	1211,3	627956,09	455358,33	FS
B13rora	13,877	3	10	276	2013	64	34,51800	16	19,74060	1283,6	0,0	-67,0	1216,5	627956,77	455358,13	FS
B14u	8,903	6	5	126	2013	64	31,63860	16	24,69660	1381,4	0,0	-67,1	1314,3	624220,95	449847,82	K
B14u	12,636	3	10	276	2013	64	31,64580	16	24,68460	1377,8	0,0	-67,1	1310,7	624229,96	449860,83	K
B15h	20,884	5	5	125	2013	64	28,48260	16	30,00660	1465,9	0,0	-67,2	1398,6	620207,75	443817,57	K
B15h	11,877	3	10	276	2013	64	28,48680	16	29,99640	1462,0	0,0	-67,2	1394,8	620215,71	443825,68	K
B16u	20,721	8	5	128	2013	64	24,11940	16	40,85220	1592,7	0,0	-67,3	1525,3	611817,26	435385,28	K
B16u	11,040	7	10	280	2013	64	24,12000	16	40,85160	1589,6	0,0	-67,3	1522,3	611817,97	435385,92	K
B17s	11,516	6	5	126	2013	64	36,73440	16	28,79820	1279,7	0,0	-67,1	1212,6	620565,02	459175,01	K
B17s	17,449	3	10	276	2013	64	36,74040	16	28,79280	1275,9	0,0	-67,1	1208,8	620568,79	459186,92	K
B18q	10,911	7	5	127	2013	64	31,58220	16	0,11220	1379,0	0,0	-66,9	1312,1	643876,22	450612,06	K
B18q	19,278	2	10	275	2013	64	31,58760	16	0,11460	1375,2	0,0	-66,9	1308,3	643873,85	450621,25	K
B19q	14,348	2	10	275	2013	64	27,93180	15	55,15680	1493,2	0,0	-66,9	1426,3	648167,34	444027,63	K
BB0r	13,703	8	5	128	2013	64	22,71660	16	5,04780	1586,5	0,0	-66,9	1519,6	640691,03	433971,79	K
BB0r	12,384	2	10	275	2013	64	22,71600	16	5,04900	1582,2	0,0	-66,9	1515,4	640690,39	433971,33	K
Borah	18,373	4	6	155	2013	64	24,94800	17	20,15040	1468,3	0,0	-67,7	1400,6	580205,99	435928,41	K
Borah	10,977	6	10	279	2013	64	24,94440	17	20,15280	1479,7	0,0	-67,7	1412,0	580204,10	435922,57	K
BORTHNb	10,544	6	10	279	2013	64	25,09380	17	19,15140	1486,7	0,0	-67,7	1419,0	581000,94	436220,87	K
Br1h	17,000	31	1	31	2013	64	5,56197	16	19,50239	178,8	0,0	-65,9	113,0	630422,84	401613,14	*
Br1i	18,736	31	1	31	2013	64	5,55752	16	19,50314	178,8	0,0	-65,8	112,9	630422,59	401604,84	K
BR2j	15,268	31	1	31	2013	64	6,39811	16	22,54422	305,4	0,0	-66,0	239,3	627887,96	403061,78	K
BR2k	15,182	31	1	31	2013	64	6,39770	16	22,54718	305,2	0,0	-66,0	239,2	627885,60	403060,92	K
Br3O	13,483	31	1	31	2013	64	8,52117	16	24,12124	471,1	0,0	-66,3	404,9	626445,74	406949,80	K
Br3p	13,483	31	1	31	2013	64	8,52117	16	24,12124	471,1	0,0	-66,3	404,9	626445,74	406950,79	K
Br4C	17,403	30	1	30	2013	64	11,73462	16	22,12542	638,9	-1,4	-66,5	571,0	627815,34	412982,78	FS
Br4d	19,460	30	1	30	2013	64	10,93446	16	20,23446	611,9	-1,3	-66,4	544,2	629407,97	411561,47	FS
Br7q	15,959	8	5	128	2013	64	22,14120	16	16,94400	1313,8	0,0	-67,0	1246,7	631176,70	432477,69	K
Br7q	11,269	3	10	276	2013	64	22,11780	16	16,93800	1309,0	0,0	-67,0	1242,0	631183,53	432434,86	K
Brur	19,391	6	5	126	2013	64	41,00160	15	55,22340	843,5	0,0	-66,7	776,8	646931,46	468280,21	K
Brur	18,557	2	10	275	2013	64	41,00220	15	55,22280	836,9	0,0	-66,7	770,1	646931,59	468280,85	K
Budr	20,882	6	5	126	2013	64	35,98920	15	59,89440	1202,6	0,0	-66,9	1135,7	643661,96	458799,42	K
Budr	19,032	2	10	275	2013	64	35,99760	15	59,89260	1198,3	0,0	-66,9	1131,4	643662,55	458814,78	K
D05q	16,214	5	5	125	2013	64	42,22080	16	54,62700	1268,7	0,0	-67,4	1201,3	599640,94	468613,23	K
D05q	11,691	4	10	277	2013	64	42,22740	16	54,61740	1264,0	0,0	-67,4	1196,7	599648,26	468624,90	FS

D07q	16,911	5	5	125	2013	64	38,28300	16	59,25180	1436,6	0,0	-67,5	1369,1	596199,51	461181,21	K
D07q	11,179	4	10	277	2013	64	38,29440	16	59,24100	1433,5	0,0	-67,5	1366,0	596207,36	461201,82	FS
D09p	13,686	5	5	125	2013	64	31,80060	17	0,54540	1647,5	0,0	-67,6	1579,9	595548,64	449110,28	K
D09p	10,758	4	10	277	2013	64	31,80480	17	0,54720	1644,8	0,0	-67,6	1577,2	595546,90	449117,24	K
D12q	12,519	5	5	125	2013	64	28,98420	17	0,13500	1713,6	0,0	-67,6	1646,1	596041,82	443890,43	K
D12q	18,526	3	10	276	2013	64	28,98480	17	0,13500	1711,0	0,0	-67,6	1643,4	596041,95	443891,19	K
E01r	18,101	7	5	127	2013	64	41,45280	15	33,49620	752,1	0,0	-66,7	685,5	664146,60	470007,86	K
E01r	17,697	2	10	275	2013	64	41,45280	15	33,49620	745,6	0,0	-66,7	679,0	664146,57	470008,02	K
E02r	17,247	7	5	127	2013	64	39,13500	15	35,97720	1021,1	0,0	-66,8	954,3	662408,14	465601,37	K
E02r	17,379	2	10	275	2013	64	39,14220	15	35,97300	1016,0	0,0	-66,8	949,3	662410,52	465614,47	K
E03s	16,557	7	5	127	2013	64	36,66660	15	36,91440	1254,6	0,0	-66,9	1187,7	661907,98	460981,44	K
E03s	17,037	2	10	275	2013	64	36,67080	15	36,91680	1249,6	0,0	-66,9	1182,7	661905,61	460989,35	K
E04r	15,884	7	5	127	2013	64	34,94940	15	37,10160	1355,6	0,0	-66,8	1288,7	661929,72	457787,21	K
E04r	16,804	2	10	275	2013	64	34,95000	15	37,10040	1351,5	0,0	-66,8	1284,6	661930,27	457788,54	K
Fl01d	12,062	8	5	128	2013	64	25,99920	15	55,30800	1396,9	0,0	-66,8	1330,1	648220,81	440435,12	K
Fl01d	13,794	2	10	275	2013	64	25,99140	15	55,29120	1391,3	0,0	-66,8	1324,5	648234,97	440422,13	K
G02j	19,610	2	6	153	2013	64	26,85180	17	17,72100	1627,8	0,0	-67,7	1560,1	582061,80	439516,78	K
G02j	16,850	4	10	277	2013	64	26,84940	17	17,72340	1625,6	0,0	-67,7	1557,9	582060,08	439511,99	FS
G03k	18,864	2	6	153	2013	64	28,43880	17	16,35360	1722,2	0,0	-67,7	1654,5	583077,87	442493,64	K
G03k	16,450	4	10	277	2013	64	28,43880	17	16,35360	1720,1	0,0	-67,7	1652,3	583077,41	442491,63	K
G04r	18,542	2	6	153	2013	64	30,02640	17	15,05460	1751,9	0,0	-67,7	1684,1	584037,42	445471,27	K
G04r	11,614	4	10	277	2013	64	30,02640	17	15,05400	1749,6	0,0	-67,7	1681,9	584037,64	445471,80	FS
GaltLon	13,949	6	6	157	2013	64	40,48260	16	41,58720	1714,6	0,0	-67,3	1647,2	610117,63	465745,28	K
GengSig	15,305	6	6	157	2013	64	40,25280	16	41,07840	1697,1	0,0	-67,3	1629,8	610538,18	465333,77	K
gb2rorb	10,050	7	5	127	2013	64	34,10640	16	0,02400	1267,9	0,0	-66,9	1201,0	643724,41	455299,52	K
gb2rorb	19,779	2	10	275	2013	64	34,11300	16	0,02580	1263,4	4,4	-66,9	1200,8	643722,64	455312,27	K
gb2c	10,050	7	5	127	2013	64	34,10640	16	0,02400	1267,9	-0,4	-66,9	1200,6	643724,41	455299,52	K
gb2c	19,779	2	10	275	2013	64	34,11300	16	0,02580	1263,4	0,0	-66,9	1196,5	643722,64	455312,27	K
Go1q	18,237	2	6	153	2013	64	33,97680	17	24,94500	1824,8	0,0	-67,8	1757,0	575935,13	452600,41	K
Go1q	12,696	4	10	277	2013	64	33,97560	17	24,94380	1822,8	0,0	-67,8	1754,9	575935,98	452598,21	FS
GvK4-1a	22,830	6	6	157	2013	64	27,56640	17	20,41140	1663,0	0,0	-67,8	1595,3	579868,78	440786,40	K
GvK4-1a	12,539	6	10	279	2013	64	27,56400	17	20,41320	1660,8	0,0	-67,8	1593,1	579867,40	440781,77	K
GvK4-2a	23,153	6	6	157	2013	64	27,35820	17	20,31480	1638,1	0,0	-67,8	1570,3	579956,40	440401,50	K
GvK4-2a	12,382	6	10	279	2013	64	27,35460	17	20,31660	1636,0	0,0	-67,8	1568,2	579955,11	440395,24	K
GvK4-3a	23,271	6	6	157	2013	64	27,27720	17	20,34960	1616,2	0,0	-67,8	1548,5	579932,28	440250,63	K
GvK4-4a	23,830	6	6	157	2013	64	27,18180	17	20,37000	1593,2	0,0	-67,8	1525,5	579920,61	440073,17	K
GvK4-4a	12,079	6	10	279	2013	64	27,17940	17	20,37120	1592,5	0,0	-67,8	1524,8	579919,74	440068,60	K
GvK4-5a	0,017	7	6	158	2013	64	27,09480	17	20,48460	1595,4	0,0	-67,8	1527,6	579832,86	439908,71	K
GvK4-5a	11,807	6	10	279	2013	64	27,09300	17	20,48520	1593,7	0,0	-67,8	1526,0	579832,60	439906,04	K
GvK4-6a	0,169	7	6	158	2013	64	27,01500	17	20,60040	1587,8	0,0	-67,8	1520,1	579744,00	439758,38	K
GvK4-6a	11,676	6	10	279	2013	64	27,01380	17	20,60100	1585,7	0,0	-67,8	1517,9	579743,62	439755,99	K
GvK4-7a	0,356	7	6	158	2013	64	26,86320	17	20,78820	1575,6	0,0	-67,8	1507,9	579601,01	439472,06	K
GvK4-7a	11,525	6	10	279	2013	64	26,86200	17	20,78880	1573,5	0,0	-67,8	1505,7	579600,41	439470,36	K
GvK4-8a	23,441	6	6	157	2013	64	27,20880	17	20,58600	1618,7	0,0	-67,8	1550,9	579746,02	440118,59	K
GvK4-8a	11,919	6	10	279	2013	64	27,20640	17	20,58180	1614,4	0,0	-67,8	1546,6	579749,54	440114,07	K
GvK4-9a	23,898	6	6	157	2013	64	27,16800	17	20,13660	1606,7	0,0	-67,8	1539,0	580108,42	440052,09	K
GvK4-9a	12,218	6	10	279	2013	64	27,16500	17	20,13900	1605,0	0,0	-67,8	1537,2	580106,59	440047,23	K
Hof01k	14,694	7	5	127	2013	64	32,32260	15	35,84160	1207,0	0,0	-66,7	1140,3	663196,71	452968,30	K
Hof01k	17,232	2	10	275	2013	64	32,31720	15	35,84100	1202,8	0,0	-66,7	1136,1	663197,80	452957,81	FS
HAABm	20,500	4	6	155	2013	64	20,96760	17	24,11880	1797,1	0,0	-67,5	1729,6	577205,83	428453,17	K
HAABm	10,500	5	10	278	2013	64	20,96760	17	24,11940	1794,3	0,0	-67,5	1726,8	577205,51	428453,30	K
K01t	14,604	3	5	123	2013	64	35,26740	17	52,35120	1078,9	0,0	-67,6	1011,3	554001,87	454528,49	FS
K01t	14,696	4	10	277	2013	64	35,26800	17	52,35360	1073,6	0,0	-67,6	1006,1	553999,58	454529,56	FS
K02u	13,421	3	5	123	2013	64	34,81800	17	49,68420	1247,2	0,0	-67,6	1179,5	556145,65	453732,18	K
K02u	14,396	4	10	277	2013	64	34,81980	17	49,69320	1242,7	0,0	-67,6	1175,1	556138,64	453735,32	FS
K03t	12,714	3	5	123	2013	64	34,24740	17	46,37940	1365,2	0,0	-67,7	1297,5	558804,92	452721,67	K
K03t	14,096	4	10	277	2013	64	34,24920	17	46,39200	1361,7	0,0	-67,7	1294,0	558794,84	452725,32	FS
K04u	11,539	3	5	123	2013	64	33,21180	17	42,24960	1554,8	0,0	-67,7	1487,1	562142,61	450863,71	K
K04u	13,804	4	10	277	2013	64	33,21480	17	42,26880	1551,3	0,0	-67,7	1483,6	562126,97	450868,79	FS
K05u	10,143	3	5	123	2013	64	33,45000	17	35,43060	1748,0	0,0	-67,8	1680,2	567582,10	451423,44	K
K05u	13,408	4	10	277	2013	64	33,44760	17	35,44320	1745,5	0,0	-67,8	1677,7	567571,85	451418,48	FS
K06t	17,796	2	6	153	2013	64	38,35440	17	31,38060	2035,4	0,0	-67,9	1967,6	570605,26	460606,72	K
K06t	13,917	4	10	277	2013	64	38,35380	17	31,37940	2033,0	0,0	-67,9	1965,1	570606,22	460606,01	K

K07p	19,678	2	5	122	2013	64	29,11260	17	42,01440	1601,2	0,0	-67,7	1533,5	562487,24	443252,82	K
K07p	15,350	4	10	277	2013	64	29,11260	17	42,01560	1598,9	0,0	-67,7	1531,2	562486,19	443252,81	FS
Ln1-1a	15,627	4	6	155	2013	64	24,50160	17	12,99780	1565,7	0,0	-67,6	1498,1	585973,31	435255,84	K
Ln1-1a	17,629	4	10	277	2013	64	24,50040	17	12,99900	1563,3	0,0	-67,6	1495,6	585972,59	435253,76	FS
Ln1-2a	15,881	4	6	155	2013	64	24,74880	17	12,01020	1590,3	0,0	-67,6	1522,7	586753,71	435738,44	K
Ln1-2a	17,458	4	10	277	2013	64	24,74640	17	12,01080	1587,5	0,0	-67,6	1519,8	586753,37	435733,26	FS
Ln1-3a	16,305	4	6	155	2013	64	24,99960	17	10,99980	1596,8	0,0	-67,6	1529,2	587552,00	436226,68	K
Ln1-3a	17,287	4	10	277	2013	64	24,99660	17	11,00100	1594,2	0,0	-67,6	1526,6	587551,00	436221,49	FS
Ln1-4a	17,169	4	6	155	2013	64	25,24680	17	10,00380	1623,0	0,0	-67,6	1555,4	588338,44	436708,85	K
Ln1-4a	17,071	4	10	277	2013	64	25,24380	17	10,00560	1620,1	0,0	-67,6	1552,5	588336,83	436703,55	FS
Ln1-5a	17,000	4	6	155	2013	64	25,74840	17	7,99440	1662,9	0,0	-67,6	1595,3	589924,14	437687,42	K
Ln1-5a	16,871	4	10	277	2013	64	25,74480	17	7,99440	1660,2	0,0	-67,6	1592,6	589924,34	437681,57	FS
S01i	13,203	4	5	124	2013	64	7,00800	17	49,98300	810,2	0,0	-66,8	743,4	556861,01	402065,21	K
S01i	12,030	5	10	278	2013	64	7,00800	17	49,98360	805,0	0,0	-66,8	738,1	556860,80	402064,53	K
S02l	12,043	4	5	124	2013	64	12,15540	17	48,96960	1076,5	0,0	-67,0	1009,5	557505,05	411642,42	K
S02l	11,509	5	10	278	2013	64	12,14700	17	48,97320	1072,6	0,0	-67,0	1005,6	557502,48	411626,74	K
S04m	11,122	4	5	124	2013	64	16,20000	17	48,22140	1227,2	0,0	-67,2	1160,0	557968,08	419167,82	K
S04m	11,198	5	10	278	2013	64	16,18920	17	48,23340	1223,1	0,0	-67,2	1155,9	557958,77	419147,06	K
Skf01d	14,821	8	5	128	2013	64	17,99460	16	4,99620	1349,6	0,0	-66,6	1283,0	641137,33	425209,82	K
Skf01d	11,484	2	10	275	2013	64	17,99200	16	4,98080	1343,2	0,0	-66,6	1276,6	641149,96	425205,77	K
T01nn	18,362	1	5	121	2013	64	19,48380	18	8,23080	816,8	0,0	-67,3	749,6	541726,70	425005,27	K
T01nn	14,751	5	10	278	2013	64	19,48380	18	8,23080	810,1	0,0	-67,3	742,9	541726,80	425005,53	K
T02np	19,716	1	5	121	2013	64	19,60140	18	3,96720	1011,1	0,0	-67,3	943,8	545159,78	425272,37	K
T02np	14,486	5	10	278	2013	64	19,60140	18	3,97260	1005,8	0,0	-67,3	938,5	545155,57	425272,09	K
T03np	21,171	1	5	121	2013	64	20,20920	17	58,59900	1145,5	0,0	-67,3	1078,2	549467,51	426468,20	K
T03np	15,225	5	10	278	2013	64	20,20800	17	58,60800	1140,6	0,0	-67,3	1073,3	549460,23	426466,45	K
T04np	12,214	2	5	122	2013	64	21,34140	17	51,51960	1289,3	0,0	-67,4	1221,9	555132,75	428669,91	K
T04np	15,533	5	10	278	2013	64	21,33900	17	51,52920	1286,0	0,0	-67,4	1218,6	555124,64	428664,77	K
T05nn	15,839	5	10	278	2013	64	22,29000	17	43,00140	1407,8	0,0	-67,5	1340,4	561953,72	430563,70	K
T05rorf	13,441	2	5	122	2013	64	22,29300	17	42,99180	1412,0	0,0	-67,5	1344,5	561961,46	430568,69	K
T05rorf	15,839	5	10	278	2013	64	22,29000	17	43,00140	1407,8	3,6	-67,5	1344,0	561953,72	430563,70	K
T06np	17,798	2	5	122	2013	64	24,27600	17	36,53940	1531,6	0,0	-67,6	1464,0	567071,33	434362,44	K
T06np	16,473	5	10	278	2013	64	24,27240	17	36,54900	1528,7	0,0	-67,6	1461,1	567063,63	434355,95	K
T07no	19,076	3	5	123	2013	64	25,28940	17	31,19760	1630,2	0,0	-67,7	1562,5	571319,20	436342,25	K
T07no	17,433	5	10	278	2013	64	25,28760	17	31,20480	1626,9	0,0	-67,7	1559,2	571313,31	436338,49	K
T07rorl	17,482	5	10	278	2013	64	25,29060	17	31,23060	1627,0	0,0	-67,7	1559,3	571292,54	436343,41	K
T08np	18,048	3	5	123	2013	64	26,31300	17	27,76800	1703,8	0,0	-67,8	1636,1	574026,74	438309,60	K
T08np	15,883	4	10	277	2013	64	26,31240	17	27,76980	1701,1	0,0	-67,8	1633,4	574025,34	438308,65	FS

Appendix D: Measured surface velocity on Vatnajökull in 2013.

Site	Calendar day date	#	Calendar day date	#	# of days	translation (m)	(°)	velocity (cm/day)	(m/annum)
B07s	130508	128	131003	276	148	1,21	157	0,82	2,99
B09t	130506	126	131003	276	150	0,48	270	0,32	1,16
B10s	121010	284	130506	126	207	5,79	3	2,80	10,21
B10t	130506	126	131003	276	150	0,48	270	0,32	1,16
B11c	130506	126	131003	276	150	6,25	27	4,17	15,21
B12s	130506	126	131003	276	150	15,72	23	10,48	38,26
B13s	130506	126	131003	276	150	18,35	25	12,23	44,64
B14u	130506	126	131003	276	150	16,43	36	10,95	39,98
B15h	130505	125	131003	276	151	11,28	46	7,47	27,27
B16u	130508	128	131007	280	152	1,21	23	0,80	2,91
B17s	130506	126	131003	276	150	11,92	21	7,94	29,00
B18q	130507	127	131002	275	148	10,18	349	6,88	25,11
BB0r	130508	128	131002	275	147	1,47	221	1,00	3,65
Borah	130604	155	131006	279	124	6,94	196	5,60	20,43
BORTHNb	121013	287	131006	279	357	9,95	194	2,79	10,17
Br3O	120420	111	130131	31	285	21,79	145	7,65	27,91
Br4C	120420	111	130130	30	284	41,78	182	14,71	53,70
Br7q	130508	128	131003	276	148	43,60	174	29,46	107,54
Brur	130506	126	131002	275	149	1,21	23	0,81	2,96
Budr	130506	126	131002	275	149	15,62	5	10,49	38,27
D05q	130505	125	131004	277	152	14,41	32	9,48	34,60
D07q	130505	125	131004	277	152	22,80	22	15,00	54,74
D09p	130505	125	131004	277	152	7,91	350	5,20	19,00
D12q	130505	125	131003	276	151	1,11	0	0,74	2,69
E01r	130507	127	131002	275	148	0,00	270	0,00	0,00
E02r	130507	127	131002	275	148	13,75	14	9,29	33,90
E03s	130507	127	131002	275	148	8,01	346	5,41	19,76
E04r	130507	127	131002	275	148	1,47	41	0,99	3,62
Fl01d	130508	128	131002	275	147	19,76	137	13,44	49,06
G02j	130602	153	131004	277	124	4,84	203	3,91	14,26
G03k	130602	153	131004	277	124	0,00	270	0,00	0,00
G04r	130602	153	131004	277	124	0,48	270	0,39	1,41
gb2rorb	121009	283	130507	127	209	10,95	355	5,24	19,12
gb2rorb	130507	127	131002	275	148	12,31	353	8,32	30,35
gb2c	121009	283	130507	127	209	10,95	355	5,24	19,12
gb2c	130507	127	131002	275	148	12,31	353	8,32	30,35
Go1q	130602	153	131004	277	124	2,42	157	1,95	7,12
GvK4-1a	130606	157	131006	279	122	4,67	198	3,83	13,98
GvK4-2a	130606	157	131006	279	122	6,82	192	5,59	20,41
GvK4-4a	130606	157	131006	279	122	4,55	192	3,73	13,61
GvK4-5a	130607	158	131006	279	121	3,37	188	2,78	10,16
GvK4-6a	130607	158	131006	279	121	2,27	192	1,88	6,86
GvK4-7a	130607	158	131006	279	121	2,27	192	1,88	6,86
GvK4-8a	130606	157	131006	279	122	5,58	143	4,57	16,68
GvK4-9a	130606	157	131006	279	122	5,88	199	4,82	17,59
HAABm	130604	155	131005	278	123	0,48	270	0,39	1,43
Hof01k	130507	127	131002	275	148	10,01	177	6,77	24,69
K01t	130503	123	131004	277	154	2,21	300	1,44	5,25
K02u	130503	123	131004	277	154	7,92	295	5,14	18,77
K03t	130503	123	131004	277	154	10,60	288	6,88	25,12

K04u	130503	123	131004	277	154	16,32	290	10,59	38,67
K05u	130503	123	131004	277	154	11,00	246	7,14	26,08
K06t	130602	153	131004	277	124	1,47	139	1,18	4,31
K07p	130502	122	131004	277	155	0,96	270	0,62	2,26
Ln1-1a	130604	155	131004	277	122	2,42	203	1,99	7,25
Ln1-2a	130604	155	131004	277	122	4,47	186	3,66	13,38
Ln1-3a	130604	155	131004	277	122	5,64	190	4,62	16,87
Ln1-4a	130604	155	131004	277	122	5,74	195	4,71	17,18
Ln1-5a	130604	155	131004	277	122	6,67	180	5,46	19,95
S01i	130504	124	131005	278	154	0,49	270	0,32	1,15
S02l	130504	124	131005	278	154	15,83	191	10,28	37,51
S04m	130504	124	131005	278	154	22,22	206	14,43	52,67
Skf01d	130508	128	131002	275	147	13,32	111	9,06	33,07
T01nn	121012	286	130501	121	200	2,13	213	1,07	3,89
T01nn	130501	121	131005	278	157	0,00	270	0,00	0,00
T02np	130501	121	131005	278	157	4,35	270	2,77	10,11
T03np	130501	121	131005	278	157	7,58	253	4,83	17,63
T04np	130502	122	131005	278	156	8,91	240	5,71	20,85
T05nn	121012	286	131005	278	357	19,18	237	5,37	19,61
T05rorf	121012	286	130502	122	201	9,69	240	4,82	17,60
T05rorf	130502	122	131005	278	156	9,51	234	6,10	22,26
T06np	130502	122	131005	278	156	10,19	229	6,53	23,85
T07no	130503	123	131005	278	155	6,67	240	4,31	15,71
T07rorl	121012	286	131005	278	357	15,79	241	4,42	16,14
T08np	130503	123	131004	277	154	1,82	232	1,18	4,32

Appendix E: Melt water runoff to selected rivers in summer 2013, derived from summer balance.

ΔS: area in a given elevation range where summer balance is negative, **∑ΔS**: cumulative area above a given elevation, **ΔQ_s**: melt water runoff from a given elevation range, **$\sum\Delta Q_s$** : cumulative melt water runoff from an area above given elevation.

Tungnaá water drainage basin

Elevation (m a. s. l.)		ΔS km^2	∑ΔS km^2	ΔQ_s ($10^6 m^3$)	$\sum\Delta Q_s$ ($10^6 m^3$)
1350	1400	0,6	0,6	0,5	0,5
1300	1350	6,2	6,8	6,3	6,8
1250	1300	10,7	17,4	13,1	19,9
1200	1250	11,4	28,9	17,0	36,9
1150	1200	10,8	39,6	19,6	56,5
1100	1150	12,8	52,4	27,9	84,4
1050	1100	11,9	64,3	30,8	115,2
1000	1050	9,7	74,0	27,8	143,0
950	1000	10,8	84,8	35,0	178,0
900	950	9,0	93,7	33,9	211,8
850	900	8,3	102,0	36,1	248,0
800	850	8,6	110,6	42,2	290,1
750	800	6,3	116,9	34,5	324,7
700	750	4,2	121,0	24,2	348,9
650	700	0,5	121,6	3,3	352,2

Sylgja water drainage basin

Elevation (m a. s. l.)		ΔS km^2	∑ΔS km^2	ΔQ_s ($10^6 m^3$)	$\sum\Delta Q_s$ ($10^6 m^3$)
1300	1350	1,3	1,3	1,5	1,5
1250	1300	3,6	5,0	4,7	6,2
1200	1250	6,4	11,4	10,1	16,3
1150	1200	8,3	19,7	15,6	32,0
1100	1150	6,6	26,3	15,2	47,2
1050	1100	7,6	33,9	21,2	68,4
1000	1050	3,8	37,7	12,5	80,9
950	1000	1,5	39,2	5,3	86,2
900	950	0,6	39,8	2,1	88,3
850	900	0,0	39,8	0,0	88,4

Western Skaftá cauldron water drainage basin

Elevation (m a. s. l.)		ΔS km^2	∑ΔS km^2	ΔQ_s ($10^6 m^3$)	$\sum\Delta Q_s$ ($10^6 m^3$)
1700	1750	3,2	3,2	1,0	1,0
1650	1700	7,0	10,2	2,5	3,4
1600	1650	8,4	18,6	3,4	6,9
1550	1600	5,0	23,6	2,2	9,1
1500	1550	1,5	25,1	0,6	9,7

Eastern Skaftár cauldoron water drainage basin

Elevation (m a. s. l.)		ΔS km^2	ΣΔS km^2	ΔQ_s $(10^6 m^3)$	$\Sigma\Delta Q_s$ $(10^6 m^3)$
1750	1800	2,5	2,5	0,6	0,6
1700	1750	10,6	13,1	3,3	3,9
1650	1700	14,8	27,8	5,6	9,5
1600	1650	9,3	37,1	3,6	13,1
1550	1600	2,2	39,3	0,9	13,9

Grímsvötn water drainage basin

Elevation (m a. s. l.)		ΔS km^2	ΣΔS km^2	ΔQ_s $(10^6 m^3)$	$\Sigma\Delta Q_s$ $(10^6 m^3)$
1900	1950	0,6	0,0	0,0	0,0
1850	1900	1,3	1,3	0,0	0,0
1800	1850	1,6	2,9	0,2	0,2
1750	1800	3,9	6,9	1,0	1,2
1700	1750	15,9	22,8	5,7	6,9
1650	1700	56,4	79,1	24,3	31,2
1600	1650	30,9	110,0	17,0	48,2
1550	1600	18,7	128,6	12,1	60,3
1500	1550	16,7	145,3	12,6	72,9
1450	1500	11,6	156,9	11,0	83,9
1400	1450	15,1	172,0	18,4	102,2
1350	1400	0,6	172,6	0,7	102,9

Kaldakvísl water drainage basin

Elevation (m a. s. l.)		ΔS km^2	ΣΔS km^2	ΔQ_s $(10^6 m^3)$	$\Sigma\Delta Q_s$ $(10^6 m^3)$
1950	2000	4,8	0,0	0,0	0,0
1900	1950	12,9	0,3	0,0	0,0
1850	1900	6,4	6,5	0,3	0,3
1800	1850	6,4	12,9	0,7	1,0
1750	1800	11,7	24,6	1,9	2,9
1700	1750	21,1	45,8	5,6	8,5
1650	1700	16,7	62,4	6,9	15,5
1600	1650	14,2	76,6	7,5	23,0
1550	1600	19,4	96,0	12,0	34,9
1500	1550	27,2	123,2	17,9	52,8
1450	1500	28,5	151,7	23,0	75,8
1400	1450	23,1	174,8	23,6	99,4
1350	1400	21,6	196,4	29,6	129,0
1300	1350	21,3	217,7	38,5	167,5
1250	1300	22,6	240,3	47,8	215,3
1200	1250	22,6	262,9	54,6	269,9
1150	1200	20,2	283,1	57,0	326,8
1100	1150	18,3	301,4	61,9	388,7
1050	1100	17,2	318,6	66,6	455,3
1000	1050	14,9	333,5	65,1	520,5
950	1000	10,7	344,1	55,5	575,9
900	950	5,6	349,7	31,5	607,4
850	900	0,5	350,3	3,2	610,6

Jökulsá á Fjöllum water drainage basin

Elevation (m a. s. l.)		ΔS km^2	∑ΔS km^2	ΔQ_s (10^6m^3)	$\sum\Delta Q_s$ (10^6m^3)
2000	2050	0,0	0,0	0,0	0,0
1950	2000	8,2	0,0	0,0	0,0
1900	1950	25,6	0,4	0,0	0,0
1850	1900	18,4	18,7	1,6	1,6
1800	1850	14,6	33,3	2,5	4,2
1750	1800	22,3	55,6	5,5	9,7
1700	1750	34,2	89,8	11,1	20,8
1650	1700	79,5	169,3	31,5	52,3
1600	1650	116,5	285,8	50,5	102,8
1550	1600	100,9	386,8	50,2	153,0
1500	1550	97,7	484,6	58,1	211,2
1450	1500	85,7	570,2	62,5	273,6
1400	1450	74,3	644,5	61,6	335,2
1350	1400	60,2	704,7	61,4	396,6
1300	1350	49,1	753,8	66,4	463,0
1250	1300	52,5	806,3	92,9	556,0
1200	1250	57,4	863,7	132,2	688,2
1150	1200	54,5	918,2	157,8	846,0
1100	1150	45,9	964,2	151,1	997,1
1050	1100	34,1	998,3	123,4	1120,5
1000	1050	36,4	1034,6	143,7	1264,2
950	1000	31,5	1066,1	135,9	1400,1
900	950	26,2	1092,3	122,9	1523,0
850	900	25,4	1117,7	128,5	1651,6
800	850	20,2	1138,0	108,9	1760,5
750	800	15,2	1153,1	87,2	1847,7
700	750	1,7	1154,9	10,4	1858,1

Kreppa and Kverká water drainage basin

Elevation (m a. s. l.)		ΔS km^2	∑ΔS km^2	ΔQ_s $(10^6 m^3)$	$\sum\Delta Q_s$ $(10^6 m^3)$
1850	1900	1,0	1,1	0,3	0,3
1800	1850	4,2	5,3	0,7	1,0
1750	1800	2,8	8,1	0,6	1,6
1700	1750	3,6	11,8	1,1	2,8
1650	1700	5,0	16,8	1,7	4,5
1600	1650	37,9	54,6	14,2	18,6
1550	1600	22,6	77,3	8,6	27,2
1500	1550	14,2	91,5	6,4	33,6
1450	1500	15,4	107,0	9,3	42,9
1400	1450	19,3	126,3	16,2	59,1
1350	1400	25,2	151,5	25,7	84,8
1300	1350	20,5	172,0	24,1	108,9
1250	1300	16,4	188,4	25,8	134,7
1200	1250	18,1	206,4	36,2	170,9
1150	1200	18,2	224,6	40,2	211,1
1100	1150	17,5	242,1	42,7	253,9
1050	1100	11,6	253,7	30,5	284,4
1000	1050	14,1	267,8	40,5	324,9
950	1000	16,1	283,9	52,3	377,3
900	950	14,4	298,2	51,3	428,5
850	900	14,5	312,7	55,6	484,2
800	850	11,5	324,2	46,8	531,0
750	800	9,3	333,5	42,5	573,5
700	750	4,2	337,7	21,1	594,6
650	700	0,4	338,1	2,3	596,9

Jökulsá á Brú water drainage basin

Elevation (m a. s. l.)		ΔS km^2	∑ΔS km^2	ΔQ_s $(10^6 m^3)$	$\sum\Delta Q_s$ $(10^6 m^3)$
1600	1650	8,3	8,3	2,9	2,9
1550	1600	30,4	38,7	11,8	14,8
1500	1550	60,6	99,3	27,2	42,0
1450	1500	63,6	162,9	37,3	79,3
1400	1450	95,6	258,5	77,6	156,9
1350	1400	124,5	383,0	116,4	273,3
1300	1350	133,2	516,2	141,1	414,4
1250	1300	128,3	644,5	169,9	584,4
1200	1250	102,8	747,3	163,2	747,6
1150	1200	87,3	834,6	162,3	909,8
1100	1150	69,3	903,8	147,1	1056,9
1050	1100	61,8	965,7	149,6	1206,6
1000	1050	51,8	1017,4	145,9	1352,5
950	1000	43,4	1060,8	140,3	1492,8
900	950	34,6	1095,5	126,3	1619,0
850	900	30,4	1125,8	120,5	1739,6
800	850	29,9	1155,7	128,2	1867,8
750	800	26,8	1182,5	130,8	1998,6
700	750	19,6	1202,1	105,1	2103,8
650	700	12,3	1214,4	70,2	2173,9
600	650	0,3	1214,8	2,0	2175,9

Jökulsá á Fljótsdal water drainage basin

Elevation (m a. s. l.)		ΔS km^2	∑ΔS km^2	ΔQ_s ($10^6 m^3$)	$\sum \Delta Q_s$ ($10^6 m^3$)
1500	1550	0,0	0,0	0,0	0,0
1450	1500	0,9	1,0	1,0	1,1
1400	1450	1,9	2,9	2,1	3,2
1350	1400	2,8	5,8	3,5	6,8
1300	1350	5,2	11,0	7,3	14,0
1250	1300	15,8	26,8	25,6	39,6
1200	1250	15,9	42,7	29,5	69,1
1150	1200	17,6	60,3	37,6	106,6
1100	1150	15,1	75,4	37,2	143,8
1050	1100	12,7	88,1	36,0	179,8
1000	1050	11,9	100,0	38,3	218,0
950	1000	9,0	109,0	32,2	250,3
900	950	5,8	114,8	22,9	273,2
850	900	4,3	119,1	18,3	291,5
800	850	3,3	122,3	14,7	306,2
750	800	3,4	125,7	16,0	322,2
700	750	3,3	129,0	16,7	338,9
650	700	1,7	130,7	9,2	348,1

Hornafjarðarfljót water drainage basin

Elevation (m a. s. l.)		ΔS km^2	∑ΔS km^2	ΔQ_s ($10^6 m^3$)	$\sum \Delta Q_s$ ($10^6 m^3$)
1450	1500	1,0	1,0	1,0	1,0
1400	1450	7,4	8,4	6,9	7,9
1350	1400	12,2	20,6	12,0	19,9
1300	1350	18,3	38,9	19,1	39,0
1250	1300	36,6	75,5	44,8	83,8
1200	1250	30,2	105,7	34,4	118,2
1150	1200	20,8	126,5	23,8	142,0
1100	1150	19,8	146,2	25,4	167,4
1050	1100	15,3	161,5	23,2	190,6
1000	1050	11,7	173,2	20,6	211,2
950	1000	11,1	184,2	22,7	233,9
900	950	8,2	192,4	19,2	253,2
850	900	5,5	198,0	14,5	267,7
800	850	4,4	202,4	12,4	280,1
750	800	4,1	206,5	12,4	292,5
700	750	4,0	210,5	12,8	305,3
650	700	3,5	213,9	12,0	317,3
600	650	2,6	216,5	9,6	326,9
550	600	2,0	218,5	8,0	335,0
500	550	1,8	220,4	7,8	342,8
450	500	1,4	221,8	6,7	349,5
400	450	1,3	223,0	6,6	356,1
350	400	0,8	223,8	4,5	360,7
300	350	1,1	225,0	6,9	367,6
250	300	2,3	227,3	15,6	383,1
200	250	3,5	230,8	24,6	407,8
150	200	2,7	233,5	20,3	428,1
100	150	2,1	235,6	17,2	445,3
50	100	2,8	238,4	23,1	468,4
0	50	0,6	239,0	4,7	473,1

Jökulsá á Breiðamerkursandi water drainage basin

Elevation (m a. s. l.)		ΔS km²	∑ΔS km²	ΔQ_s ($10^6 m^3$)	$\sum\Delta Q_s$ ($10^6 m^3$)
1700	1750	0,8	0,8	0,3	0,3
1650	1700	4,0	4,9	1,4	1,6
1600	1650	12,9	17,8	4,6	6,2
1550	1600	19,1	36,8	7,3	13,5
1500	1550	23,0	59,8	11,0	24,6
1450	1500	35,2	95,0	22,3	46,9
1400	1450	49,6	144,6	36,6	83,6
1350	1400	83,3	227,9	69,9	153,5
1300	1350	85,4	313,2	74,0	227,5
1250	1300	53,1	366,4	48,9	276,4
1200	1250	35,1	401,5	35,3	311,7
1150	1200	28,9	430,3	33,8	345,5
1100	1150	24,6	454,9	34,6	380,1
1050	1100	20,7	475,6	34,6	414,7
1000	1050	17,8	493,4	34,2	448,9
950	1000	19,0	512,4	40,6	489,5
900	950	20,2	532,6	47,8	537,3
850	900	20,5	553,2	54,5	591,7
800	850	20,2	573,3	57,3	649,1
750	800	19,5	592,9	59,9	708,9
700	750	21,1	614,0	69,5	778,4
650	700	26,7	640,6	92,8	871,2
600	650	18,5	659,1	68,4	939,5
550	600	18,5	677,7	72,1	1011,7
500	550	7,0	684,7	28,7	1040,3
450	500	7,7	692,3	36,5	1076,8
400	450	5,8	698,2	30,6	1107,4
350	400	5,5	703,6	30,7	1138,2
300	350	6,5	710,2	39,6	1177,7
250	300	6,0	716,1	39,9	1217,6
200	250	6,3	722,5	46,7	1264,4
150	200	5,1	727,6	40,5	1304,9
100	150	5,1	732,7	42,0	1346,9
50	100	4,1	736,8	34,7	1381,5
0	50	2,7	739,5	22,9	1404,5

Breiðárlón/Fjallsárlón water drainage basin

Elevation (m a. s. l.)		ΔS km^2	∑ΔS km^2	ΔQ_s ($10^6 m^3$)	$\sum \Delta Q_s$ ($10^6 m^3$)
1900	1950	0,1	0,3	0,0	0,0
1850	1900	1,4	1,8	0,0	0,0
1800	1850	2,1	3,9	0,2	0,3
1750	1800	2,5	6,4	0,5	0,8
1700	1750	2,9	9,3	0,8	1,6
1650	1700	2,9	12,2	1,0	2,6
1600	1650	4,0	16,2	1,8	4,4
1550	1600	4,2	20,4	2,3	6,7
1500	1550	6,0	26,4	3,8	10,5
1450	1500	5,0	31,4	3,4	13,9
1400	1450	5,3	36,7	3,9	17,8
1350	1400	6,4	43,1	5,3	23,2
1300	1350	12,6	55,7	10,9	34,1
1250	1300	6,7	62,5	6,3	40,4
1200	1250	5,6	68,0	5,9	46,3
1150	1200	5,1	73,1	6,1	52,4
1100	1150	4,5	77,6	6,4	58,9
1050	1100	5,0	82,6	7,9	66,7
1000	1050	6,0	88,6	10,4	77,1
950	1000	7,0	95,6	14,7	91,8
900	950	8,4	104,0	19,5	111,4
850	900	6,7	110,7	17,4	128,8
800	850	8,4	119,1	23,6	152,4
750	800	8,8	127,9	27,0	179,4
700	750	6,1	134,1	20,1	199,5
650	700	7,4	141,5	26,1	225,6
600	650	8,3	149,8	31,1	256,6
550	600	8,8	158,6	34,9	291,6
500	550	9,5	168,1	40,4	331,9
450	500	9,6	177,7	44,5	376,5
400	450	11,1	188,8	56,5	433,0
350	400	8,5	197,3	47,8	480,8
300	350	7,7	205,0	46,4	527,2
250	300	7,4	212,4	49,1	576,4
200	250	6,8	219,2	48,5	624,9
150	200	4,6	223,8	35,8	660,7
100	150	4,3	228,1	35,2	695,9
50	100	3,7	231,8	30,8	726,7
0	50	1,8	233,6	15,4	742,2

Skeiðarársandur water drainage basin (Gígja)

Elevation (m a. s. l.)		ΔS km^2	∑ΔS km^2	ΔQ_s ($10^6 m^3$)	$\sum\Delta Q_s$ ($10^6 m^3$)
1700	1750	1,2	1,2	0,4	0,4
1650	1700	20,5	21,7	8,3	8,7
1600	1650	76,2	97,9	30,0	38,7
1550	1600	84,6	182,5	36,1	74,9
1500	1550	104,1	286,7	47,6	122,5
1450	1500	97,6	384,3	50,7	173,2
1400	1450	95,1	479,3	58,6	231,8
1350	1400	83,3	562,6	62,4	294,3
1300	1350	71,9	634,5	62,9	357,2
1250	1300	62,8	697,3	63,2	420,4
1200	1250	52,9	750,1	61,8	482,2
1150	1200	44,9	795,1	63,2	545,4
1100	1150	36,1	831,2	59,4	604,8
1050	1100	29,5	860,7	56,0	660,8
1000	1050	25,0	885,7	53,0	713,9
950	1000	25,0	910,7	58,4	772,3
900	950	24,8	935,5	63,9	836,2
850	900	27,8	963,3	78,6	914,8
800	850	22,5	985,7	69,3	984,1
750	800	19,6	1005,3	65,5	1049,6
700	750	19,1	1024,4	68,3	1117,9
650	700	11,9	1036,3	45,3	1163,2
600	650	13,1	1049,4	53,5	1216,7
550	600	12,4	1061,8	52,1	1268,8
500	550	8,3	1070,1	35,9	1304,7
450	500	5,5	1075,6	26,2	1330,9
400	450	6,7	1082,3	35,2	1366,1
350	400	11,1	1093,4	62,8	1428,9
300	350	14,2	1107,6	87,0	1515,8
250	300	15,3	1122,9	99,9	1615,8
200	250	12,4	1135,3	87,3	1703,1
150	200	11,3	1146,6	85,2	1788,3
100	150	13,5	1160,1	108,6	1896,9
50	100	5,0	1165,1	41,7	1938,6

Súla water drainage basin

Elevation (m a. s. l.)		ΔS km^2	∑ΔS km^2	ΔQ$_s$ (10^{6}m^3)	∑ΔQ$_s$ (10^{6}m^3)
1700	1750	0,5	0,5	0,2	0,2
1650	1700	1,4	2,0	0,5	0,7
1600	1650	2,6	4,5	1,1	1,8
1550	1600	4,1	8,6	2,0	3,8
1500	1550	5,9	14,6	3,1	6,9
1450	1500	11,4	26,0	6,7	13,6
1400	1450	11,1	37,1	7,6	21,2
1350	1400	9,3	46,4	7,7	28,8
1300	1350	8,2	54,6	7,6	36,4
1250	1300	6,7	61,3	7,0	43,4
1200	1250	8,1	69,3	9,6	53,0
1150	1200	9,2	78,5	12,7	65,7
1100	1150	15,6	94,1	24,5	90,1
1050	1100	15,9	110,0	29,2	119,3
1000	1050	16,5	126,5	34,7	154,0
950	1000	18,7	145,2	44,2	198,2
900	950	15,3	160,5	39,8	238,0
850	900	12,1	172,7	34,5	272,4
800	850	11,7	184,4	36,1	308,5
750	800	7,0	191,3	23,5	332,1
700	750	6,0	197,4	21,8	353,8
650	700	4,9	202,3	18,8	372,6
600	650	9,0	211,3	36,6	409,2
550	600	11,7	223,0	49,6	458,9
500	550	8,9	231,9	38,9	497,8
450	500	7,2	239,1	33,4	531,2
400	450	6,3	245,4	32,3	563,5
350	400	4,8	250,2	26,9	590,4
300	350	1,8	252,0	11,0	601,4
250	300	0,9	252,9	6,2	607,6
200	250	0,8	253,7	5,4	613,0
150	200	0,8	254,5	6,0	619,0
100	150	0,8	255,3	6,7	625,7
50	100	0,6	256,0	5,5	631,2

Djúpá water drainage basin

Elevation (m a. s. l.)		ΔS km^2	∑ΔS km^2	ΔQ_s ($10^6 m^3$)	$\sum\Delta Q_s$ ($10^6 m^3$)
1450	1500	0,1	0,1	0,1	0,1
1400	1450	0,3	0,5	0,3	0,4
1350	1400	0,9	1,4	1,0	1,4
1300	1350	3,8	5,1	4,0	5,4
1250	1300	3,3	8,5	4,1	9,5
1200	1250	2,9	11,4	3,8	13,3
1150	1200	3,5	14,9	5,1	18,4
1100	1150	5,3	20,3	8,9	27,3
1050	1100	7,0	27,3	14,6	41,8
1000	1050	9,8	37,1	24,5	66,4
950	1000	8,0	45,1	23,0	89,4
900	950	8,1	53,2	25,0	114,4
850	900	7,5	60,7	24,7	139,1
800	850	9,1	69,8	32,0	171,1
750	800	6,7	76,5	24,9	195,9
700	750	4,0	80,6	15,9	211,8
650	700	3,0	83,5	12,1	224,0
600	650	0,4	84,0	1,8	225,7

Brunná water drainage basin

Elevation (m a. s. l.)		ΔS km^2	∑ΔS km^2	ΔQ_s ($10^6 m^3$)	$\sum\Delta Q_s$ ($10^6 m^3$)
1050	1100	0,0	0,0	0,2	0,2
1000	1050	1,1	1,2	2,9	3,1
950	1000	3,3	4,5	9,5	12,5
900	950	4,2	8,6	13,1	25,7
850	900	4,3	13,0	14,6	40,2
800	850	4,9	17,8	17,2	57,5
750	800	5,4	23,3	20,1	77,5
700	750	6,4	29,6	24,7	102,2
650	700	3,9	33,5	16,1	118,3
600	650	2,3	35,9	10,2	128,5
550	600	0,0	35,9	0,1	128,7

Hverfisfljót water drainage basin

Elevation (m a. s. l.)		ΔS km^2	ΣΔS km^2	ΔQ_s ($10^6 m^3$)	$\Sigma\Delta Q_s$ ($10^6 m^3$)
1700	1750	0,8	0,8	0,2	0,2
1650	1700	5,1	5,9	1,9	2,2
1600	1650	9,1	15,0	3,6	5,7
1550	1600	9,0	24,0	3,6	9,4
1500	1550	19,7	43,7	8,7	18,1
1450	1500	42,0	85,8	21,6	39,7
1400	1450	28,5	114,3	18,1	57,8
1350	1400	24,5	138,8	19,9	77,7
1300	1350	22,9	161,6	22,4	100,1
1250	1300	18,6	180,2	21,0	121,1
1200	1250	20,2	200,4	25,6	146,6
1150	1200	14,1	214,5	20,4	167,0
1100	1150	10,9	225,4	19,2	186,2
1050	1100	10,2	235,6	21,6	207,8
1000	1050	9,3	244,8	23,0	230,8
950	1000	9,4	254,2	26,8	257,6
900	950	8,9	263,2	28,2	285,8
850	900	7,4	270,5	25,1	310,9
800	850	9,3	279,8	32,9	343,8
750	800	11,5	291,3	42,4	386,2
700	750	13,7	305,0	52,9	439,1
650	700	7,8	312,8	32,1	471,2
600	650	4,6	317,3	19,6	490,8
550	600	0,2	317,5	0,8	491,6

Skaftá water drainage basin

Elevation (m a. s. l.)		ΔS km^2	ΣΔS km^2	ΔQ_s ($10^6 m^3$)	$\Sigma\Delta Q_s$ ($10^6 m^3$)
1650	1700	2,9	2,9	1,3	1,3
1600	1650	16,1	19,0	6,9	8,2
1550	1600	23,8	42,8	10,2	18,3
1500	1550	29,5	72,2	13,8	32,1
1450	1500	24,1	96,3	12,3	44,4
1400	1450	22,4	118,7	14,2	58,7
1350	1400	20,7	139,4	16,8	75,4
1300	1350	22,9	162,3	22,9	98,3
1250	1300	16,4	178,7	19,5	117,9
1200	1250	21,5	200,2	29,6	147,5
1150	1200	23,9	224,2	38,6	186,0
1100	1150	24,5	248,7	47,1	233,1
1050	1100	26,8	275,5	60,8	293,9
1000	1050	26,3	301,8	69,2	363,0
950	1000	20,3	322,1	61,5	424,5
900	950	15,8	337,9	54,1	478,6
850	900	16,2	354,1	62,9	541,5
800	850	14,7	368,8	64,6	606,2
750	800	11,6	380,4	55,3	661,4
700	750	8,5	388,9	43,4	704,8
650	700	5,1	394,0	26,4	731,2
600	650	0,9	394,9	4,9	736,1

Appendix F: MODIS satellite images of Vatnajökull and vicinity 2012-2013.

Left: September 2nd (western half) September 7th (eastern half) 2012; abrupt end of summer, obvious snowfall in the upper regions. Right: September 20th, winter conditions, September to mid-October with high winds and precipitation.

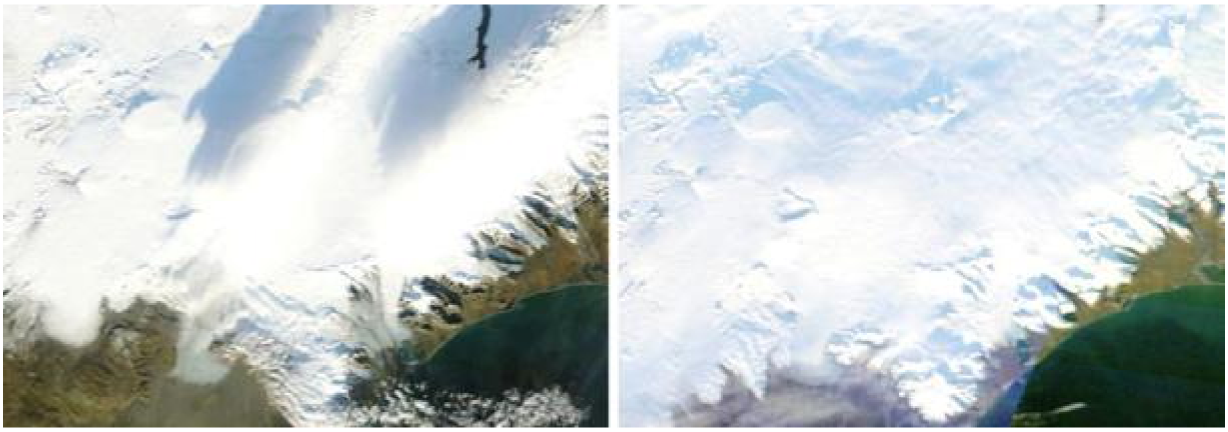

Left: October 31st, snow in the highlands above ~600m. Right: November 19th, the snowline is migrating downwards, now at ~200 m.

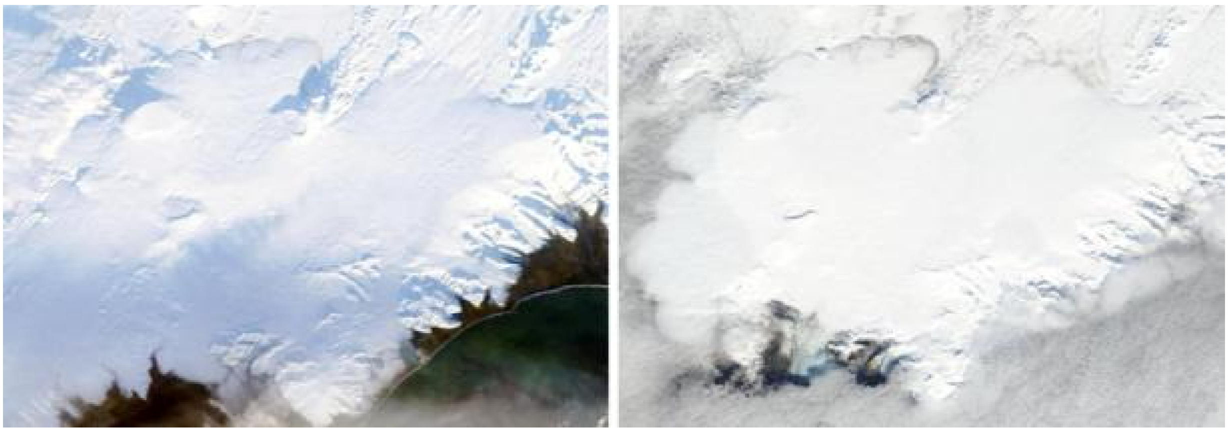

Left: January 25th 2013, no obvious change since mid-November 2012. Right: March 10th, the snow cover in the highland and snouts of the northern and western outlets is very thin; some of the winter snow has already melted.

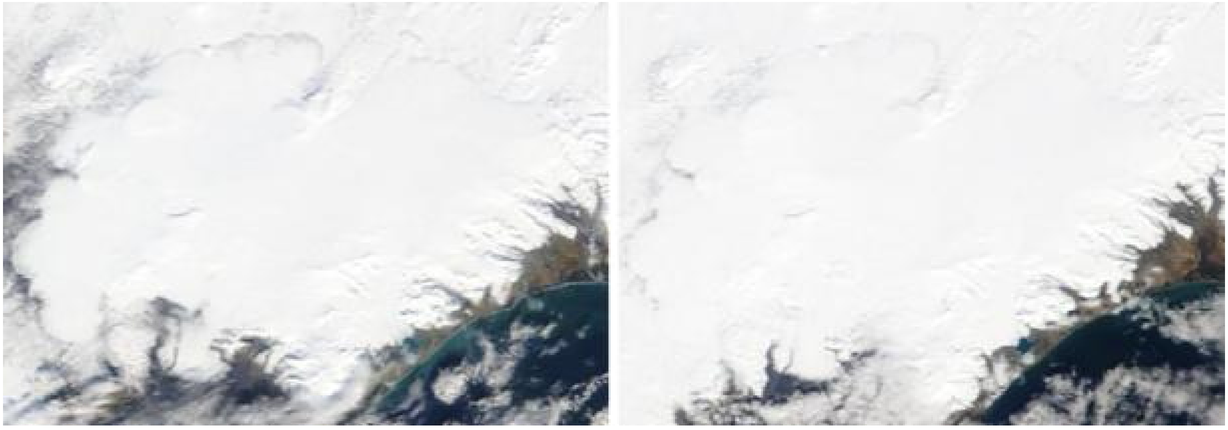

Left: March 25th. Right: April 26th. No obvious change since March 10th, except fresh snow in the north highland.

Left: May 21st, this late in May there is still some snow in the lowest parts of Breiðamerkurjökull, in May there is no cloud-free image of Vatnajökull. Right: June 6th, onset of summer conditions, melt season has started,

Left: June 16th, visible changes from June 6th are small, seemingly there has not much melt these 10 days, Dirt blown from the frontal areas are visible on the surface of Brúarjökull. Right: June 23rd, this is mid-summer and still there is little melt, the snowline has migrated slightly upwards on most outlets. The dirt on Dyngjujökull and Brúarjökull has increased, this will enhance melt in coming weeks.

Left: July 9th, more dirt on Brúarjökull and Dyngjujökull, snowline has moved upwards significantly. Right: July 28th, the warmest and sunniest period of summer, high melt rates on all outlets.

Left: August 12th, the snow line has only migrated slightly over two weeks, fresh snow in the western accumulation zone. Right: August 26th, the snowline of the NE-outlets has raised significantly; a warm and sunny period in NE-Iceland.

Left: September 7th, fresh snow in most accumulation zones, and even the ablation zones of the western part, frequent low pressure systems pass Iceland; onset of winter. Right: September 24th, clear winter conditions, snow accumulation has started.

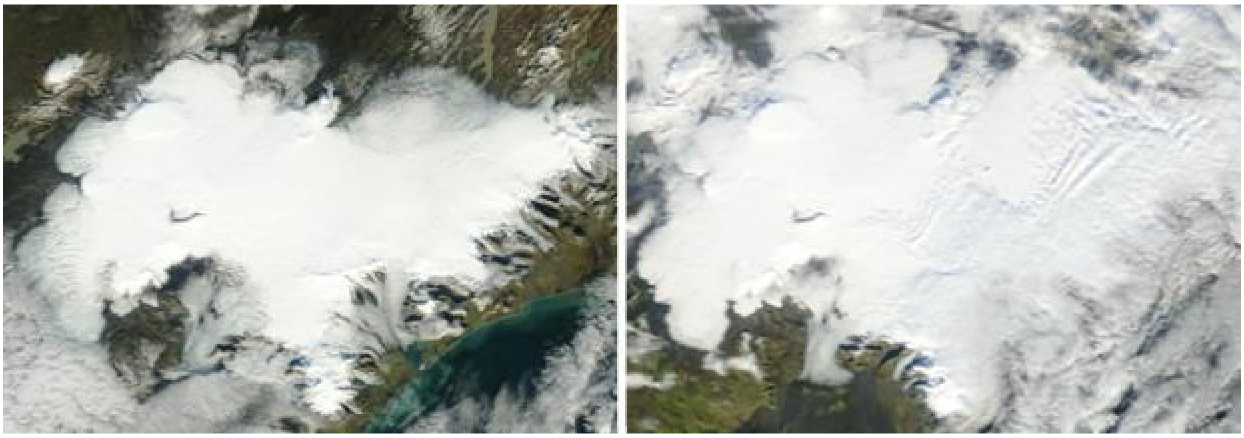

Left: October 14th, the first cloud-free image since September 24th. Some of the fresh snow has melted in the ablation zone; however snow cover up to 1.2 m was measured in the autumn mass balance expedition (October 1-8th) in the upper region. Right October 19th. Winter has settled in.

The images are either from the MODIS Aqua or MODIS Terra satellites, visible light, 250m resolution.
http://rapidfire.sci.gsfc.nasa.gov/

The Moderate Resolution Imaging Spectroradiometer (MODIS) flies onboard NASA's Aqua and Terra satellites as part of the NASA-centered international Earth Observing System. Both satellites orbit the Earth from pole to pole, seeing most of the globe every day. Onboard Terra, MODIS sees the Earth during the morning, while Aqua MODIS orbits the Earth in the afternoon.

On the next pages MODIS images for all days of May, June, July, August and September 2013 are shown.

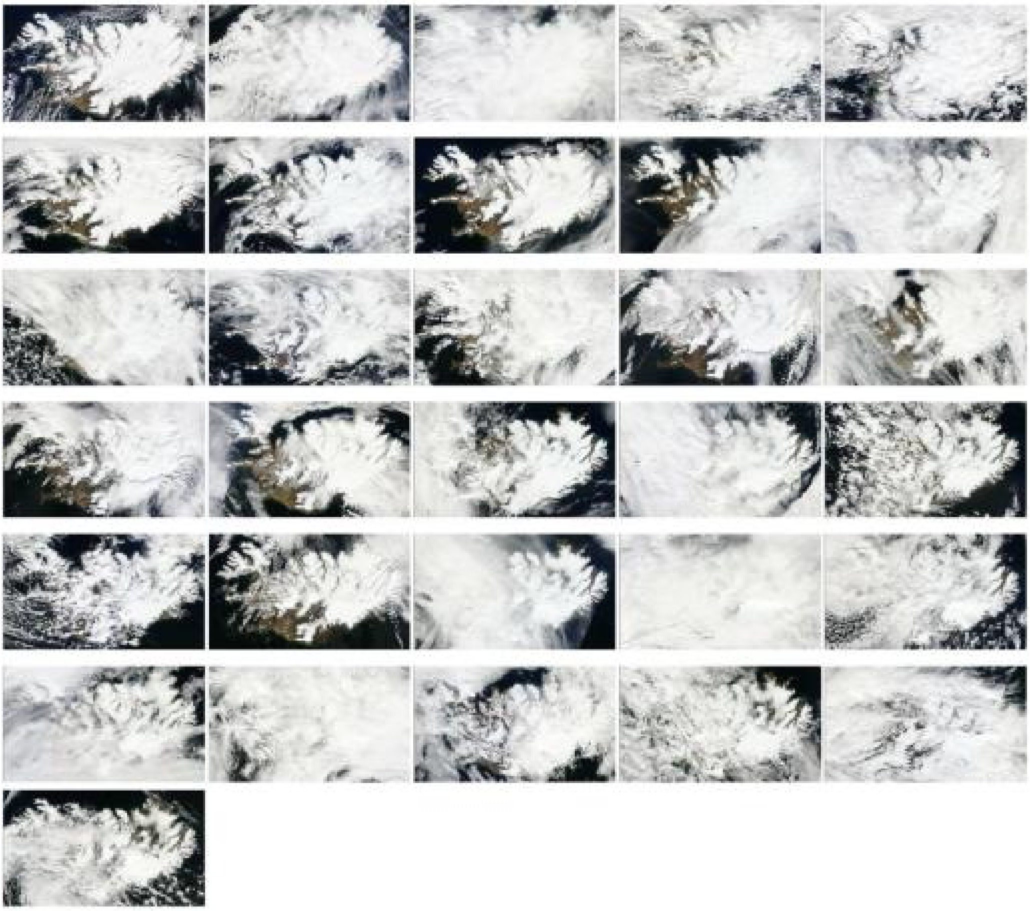

MODIS: May 2013 (read from left to right and downwards).

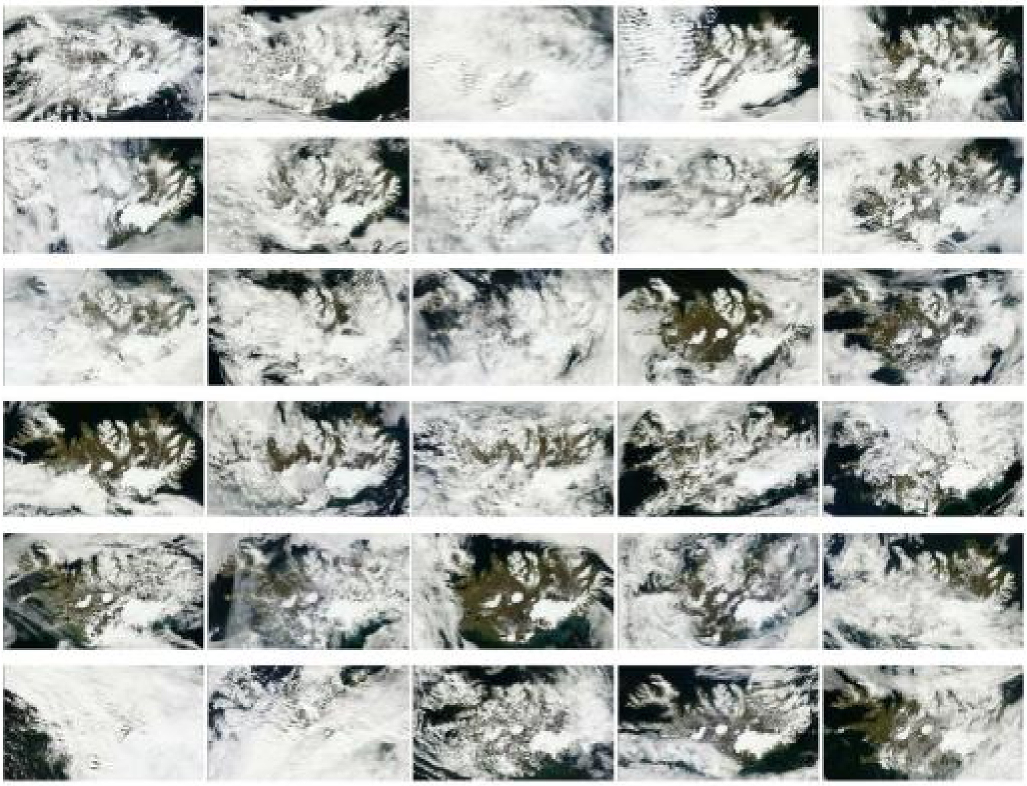

MODIS: June 2013 (read from left to right and downwards).

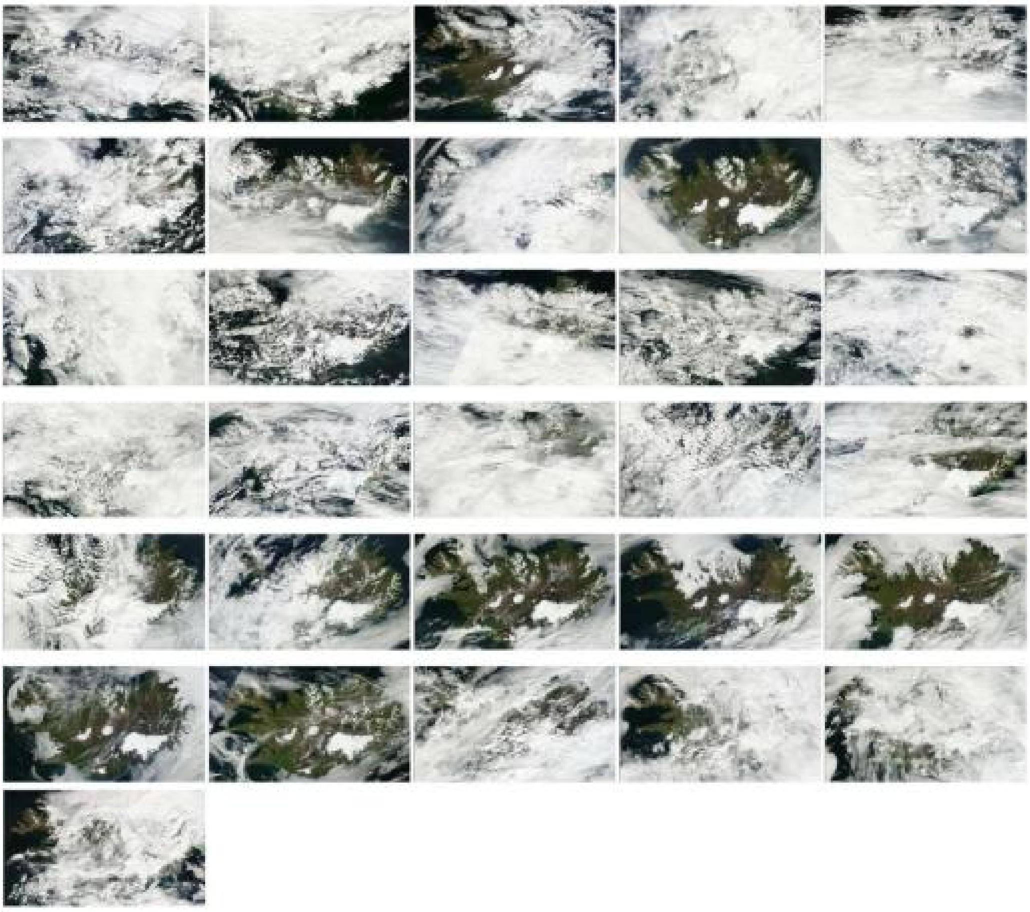

MODIS: July 2013 (read from left to right and downwards).

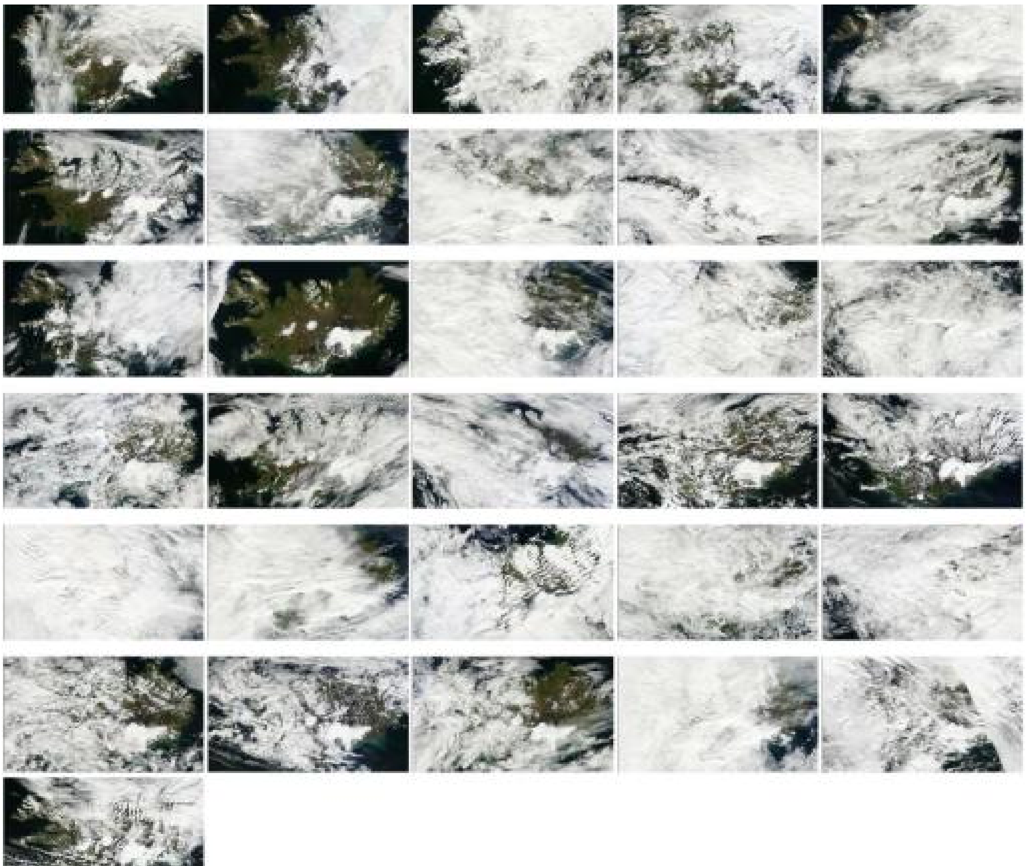

MODIS: August 2013 (read from left to right and downwards).

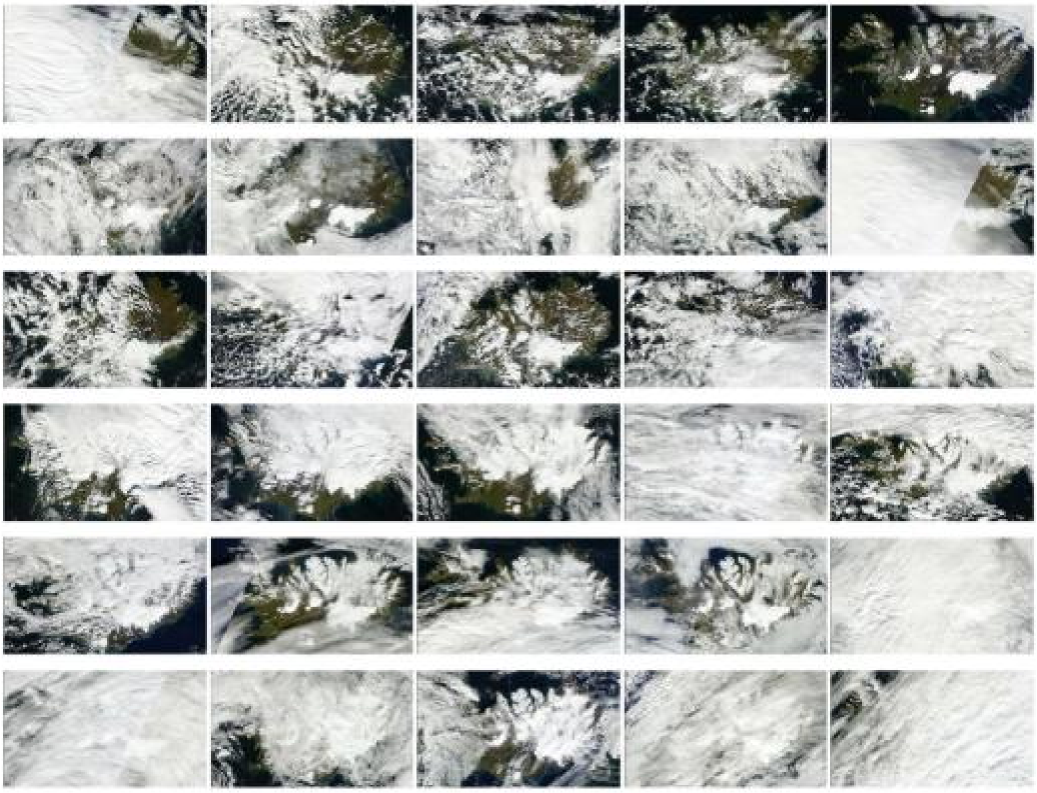

MODIS: September 2013 (read from left to right and downwards).